INVESTIGATION INTO NARROWER SLOT OF DUMBBELL SHAPE DEFECTED GROUND STRUCTURE UNDER A STANDARD MICROSTRIP T-LINE

by

Md. Amir Hossain

A thesis submitted in partial fulfillment of the requirement for the degree of
Master of Science in Electrical and Electronic Engineering

Supervised by

Prof. Dr. Md. Nurunnabi Mollah

Department of Electrical and Electronic Engineering
Khulna University of Engineering & Technology
Khulna -9203, Bangladesh.

January -2019

Declaration

This is to certify that the thesis work entitled *"**Investigation into narrower slot of dumbbell shape defected ground structure under a standard microstrip T-line**"* has been carried out by **Md. Amir Hossain** in the *Department of Electrical and Electronic Engineering*, Khulna University of Engineering and Technology, Khulna, Bangladesh. The above thesis work or any part of this work has not been submitted anywhere for the award of any degree or diploma.

17.01.19
Signature of the Supervisor

17.01.19
Signature of the Candidate

Approval

This is to certify that the thesis work submitted by *Md. Amir Hossain* entitled, "*Investigation into narrower slot of dumbbell shape defected ground structure under a standard microstrip T-line*" has been approved by the board of examiners for the partial fulfillment for the degree of *Master of Science in Electrical & Electronic Engineering* in the Department of *Electrical and Electronic Engineering,* Khulna University of Engineering & Technology, Khulna, Bangladesh in January, 2019.

Board of Examiners

1. 17.01.19
Dr. Md. Nurunnabi Mollah
Professor
Department of Electrical & Electronic Engineering
Khulna University of Engineering & Technology
— Chairman (Supervisor)

2. 17-1-19
Head
Department of Electrical & Electronic Engineering
Khulna University of Engineering & Technology
— Member

3. 17/1/2019
Prof. Dr. Mohammad Shaifur Rahman
Department of Electrical & Electronic Engineering
Khulna University of Engineering & Technology
— Member

4. 17.01.2019
Dr. Md. Jahirul Islam
Assistant Professor,
Department of Electrical & Electronic Engineering
Khulna University of Engineering & Technology
— Member

5. 17.01.19
Prof. Dr. Mohammad Ismat Kadir
ECE Discipline,
Khulna University, Khulna
— Member (External)

Acknowledgement

Alhamdulillah (All praise be to Allah), the Cherisher and Sustainer of the world, the most Gracious, the most Merciful for enabling me to complete this analysis and research for investigation into dumbbell shape defected ground structure thesis.

First and foremost, I would like to present my deepest appreciation and gratitude to my supervisor **Dr. Md. Nurunnabi Mollah**, Professor, Department of Electrical and Electronic Engineering Khulna University of Engineering & Technology (KUET) for his scholastic guidance, constructive suggestion, valuable advices and all the possibilities and opportunities, he has provided me with throughout my graduate life. I am very glad to have found the chance to work with him. Completing this thesis could not be possible without his kind co-operation cordial help. I also thank my Head of the Department and board members for their co-operations. I am grateful who have helped me to complete my work.

I would like to thank my friends and staff members for their exceptional support, encouragement, help and patience during this study.

Finally, I would like to thank the members of my family for their support during this study.

17.01.19

Md. Amir Hossain

Abstract

Electromagnetic Band Gap Structures (EBGSs) delivered a wide assortment of plan choices for specialists working in the territory of microwave and photonics. The spotlight is currently towards on discovering genuine applications. Because of the unbelievable capability of EBGSs, there are enormous applications in which they can be utilized.

This thesis describes the planar EBG structures in the forms of conventional circular and rectangular EBGSs and dumbbell-shaped defected ground structures (DS-DGSs). Conventionally, the DS- DGS consists of two bigger slots and a narrower slot. Here the shape of narrower slot of dumbbell shape DGS has been focused. Modified EBGS in the form of changing the gap height of narrower slots of dumbbell-shaped DGS cells has been studied. These modified DGSs provide wide stopband properties. The DS-DGSs study has been carried out with the investigation into narrower slots and their properties. Some modified designs have been proposed such as; changing the height and width of the narrower slot of the dumbbell-shaped DGSs we have seen the performance. We have also increased the number of narrower slot to see the performance. The modified designs perform better than the conventional DGSs reported in the open literature. The proposed DGSs yield lowpass filter (LPF) properties with good passband and amazingly wide stopband.

In this thesis, uniform circular and rectangular with different filling factor (FF) and DS-DGS with similar periodicity like circular or rectangular structure have investigated. Then for the better performance, we have focused on narrower slot of the DS-DGSs. This research conveys the performance of filter at about 4 GHz cutoff frequency. These distributions remove the unwanted spurious transmission in the band rejection region. It is seen that in the dumbbell shape DGS the number of the narrower slot has a significant role to control the depth and width of the stopband. Besides, the optimized design is achieved by varying the height of the narrower slot. For two narrower slots, it provides the best performance. The optimized design has the size of the larger slot of 5.22×5.22 sq mm and the narrower slot is 0.78×0.75 sq mm. The proposed DS-DGS with two narrower slots is suitable for lowpass filter implementation.

Finally, the insertion loss (IL) and return loss (RL) performances of different designs have been compared. It is seen that our modified designs provide improved performance and more compactness in terms of return and insertion-loss bandwidths. The sufficient explanations have been provided to validate the total research works.

Contents

Chapter 5: Conclusion

List of Figures

List of Tables

List of Abbreviations

EBGS	**:**	**Electromagnetic Bandgap Structure**
PBGS	**:**	**Photonic Bandgap Structure**
UPBGS	**:**	**Uniform PBGS**
UWB	**:**	**Ultra Wideband**
SAR	**:**	**Specific Absorption Rate**
FF	**:**	**Filling Factor**
BPF	**:**	**Bandpass Filter**
DGS	**:**	**Defected Ground Structures**
DS	**:**	**Dumbbell Shape**
MEMS	**:**	**Micro Electro Mechanical Systems**
CPW	**:**	**Coplanar waveguide**
AMC	**:**	**Artificial magnetic conducting**
UC-PBG	**:**	**Uniplanar compact-photonic bandgap**
EM	**:**	**Electromagnetic**
PC	**:**	**Photonic crystal**
1-D, 2-D, 3-D	**:**	**One-dimensional, two-dimensional, three-dimensional**
RF	**:**	**Radio frequency**
IL	**:**	**Insertion Loss**
RL	**:**	**Return Loss**
SWS	**:**	**Slow wave structures**
TEM	**:**	**Transverse Electromagnetic**
FDTD	**:**	**Finite Difference Time-Domain**
FEM	**:**	**Finite Element Method**
MOM	**:**	**Method of Moments**
dB	**:**	**Decibel**
BW	**:**	**Bandwidth**
LPF	**:**	**Lowpass Filter**
FSS	**:**	**Frequency Selective Surfaces**
VNA	**:**	**Vector Network Analyzer**

List of Major Symbols

ε_r	:	Dielectric constant
ε_{eff}	:	Effective relative permittivity
C_0	:	Speed of light in free space
γ	:	Propagation constant
β	:	Phase constant
ω	:	Angular frequency
k	:	Wave number (/m)
α	:	Attenuation constant
λ_g	:	Guided wavelength
λ_0	:	Wavelength in air
Z_0	:	Characteristic impedance
f_0	:	Center frequency
S	:	Scattering parameters

Chapter 1

Introduction

1.1. Electromagnetic Bandgap Structures (EBGS)

Recently EBGs engineering has an acquired area in microwave engineering. EBGSs are found to be very attractive in different enormous devices and components. For high performance of wireless communication and advanced modern technologies, the demand for large bandwidth, high efficiency radio frequency devices, ease of installation, low profile antennas with the microwave devices is tremendous. In order to meet these requirements the new technique Electromagnetic Bandgap Structures (EBGSs) have been introduced as potential means of improving the performances of existing RF active and passive devices. EBGSs are periodic structures which exhibit distinct passband and stopband properties. These are the unique properties of this structure.

On the other hand, planar photonic bandgap structures (PBGSs) are a class of periodic structure with ability to control the propagation of electromagnetic wave [1]. Electromagnetic (EM) waves behave in substrates as electrons behave in semiconductors. Due to these characteristic EBGSs are also known as electromagnetic bandgap structures (EBGSs). EBGS is also called electromagnetic crystal and exhibit a frequency-selective behavior similar to carrier transport in semiconductors. The perturbation in the ground plane of a structure is widely known as defected ground structure (DGS) [2]. When the perturbation in the ground plane is uniform, then it is known as EBGS. Also, they exhibit wide band-pass and band-rejection properties at microwave and millimeter-wave frequencies and have offered tremendous applications in active and passive devices [3-8]. They allow shifting the rejected frequency band by simply changing the geometry parameters of the EBG element.

Introducing periodic perturbation such as the dielectric rods, holes and patterns in waveguides and microstrip substrates forms EBG materials. While various configurations have been proposed in literature, only the planar etched EBG configurations are attracting much interest due to their ease of fabrication and integration with other circuits with photolithographic processes [9-12]. The sample design of EBG structure (square patterned 2-D structure beneath the transmission line) is shown in figure below. In the whole thesis we have designed all structures in the MGRID of EM software Zeland IE3D. We have simulated all designs by using MODUA platform of the same software. We have focused our investigation to see the depth and width of the rejection/band or stopband for all designs. The graphical presentations of the performances are described by the return loss (S_{11}) and insertion loss (S_{21}). The attenuated insertion loss is basically stopband performance of the design.

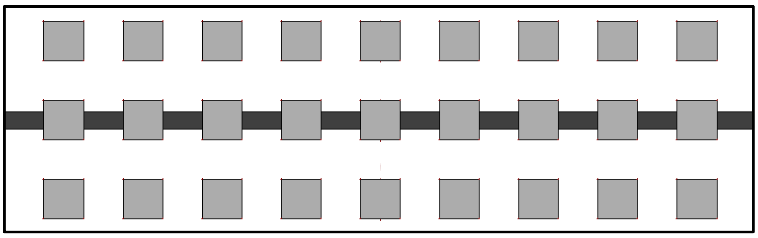

Fig 1.1. Geometry of a 3 rows (2-D) of uniform square EBGSs beneath the transmission line.

The passband of EBGSs is used as a slow wave medium that is useful for compact design. On the other hand the stopband is used to suppress the surface wave, leakage and spurious transmission [13-16]. Due to these unique properties of EBG structures, they find potential application in filter, antennas, waveguides, phased arrays and many other microwave devices and components [17].

DS-defected ground structures (DS-DGS) differs from the EBGSs, both in configuration and in principle of operations. DS-DGSs are formed from 2-D regular square patterned EBGSs with narrow vertical slot connections. They are known as DS-DGSs [2], [18]. In principle, EBGSs follow Bragg's condition to generate the stopband. On the other hand the behavior of DS-DGSs is controlled by current path around the DGS element. The unit cell of a DS-DGS is shown below:

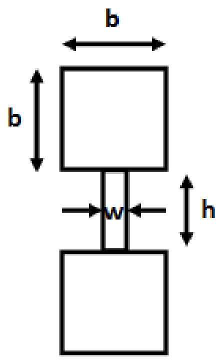

Fig 1.2. A DS-EBG structure whose length and height is b and gap width is w and gap height is h

Nonlinear distribution in EBGSs provides smoother transmission passband and DS-DGSs provide wider stopband [19-22]. These two concepts are combined to design EBGS assisted filter which will be investigated in this paper. From there we will be able to conclude that the designs are able to use as a filter.

1.2. S- Parameters

The network representation of a two-port network at high RF/microwave frequencies is called "scattering parameters" (or "S-parameters" for short). The high frequency S-parameters are used for characterizing high RF/Microwave two-port networks. These parameters are based on the concept of travelling waves and provide a complete characterization of any two-port network under analysis or test at RF/Microwave frequencies. In view of the linearity of the electromagnetic field equations and the linearity displayed by most microwave components and networks, the “scattered waves” (i.e. the reflected and transmitted wave amplitudes) are linearly related to the incident wave amplitude. The matrix describing this linear relationship is called the “scattering matrix” or [S]. S-parameters as defined above have many advantages at high RF/Microwave frequencies which can be briefly stated as:

- S-parameters provide a complete characterization of a network, as seen at its ports.
- S-parameters make the use of short or open (as prescribed at lower frequencies) completely unnecessary at higher frequencies.
- S-parameters require the use of matched loads for termination and since the loads absorb all the incident energy, the possibility of serious reflections back to the device or source is eliminated.

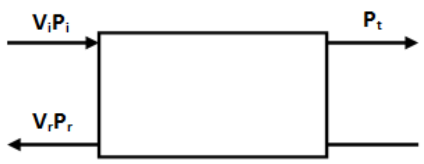

Fig 1.3. Symmetrical two-port network

$$\text{Return loss}, S_{11} = 20\ log_{10}\left(\frac{V_r}{V_i}\right)$$

$$= 10\ log_{10}\left(\frac{p_r}{p_i}\right) \qquad (1.\ 1)$$

$$\text{Insertion loss}, S_{21} = 20\ log_{10}\left(\frac{V_t}{V_i}\right)$$

$$= 10\ log_{10}\left(\frac{p_t}{p_i}\right) \qquad (1.\ 2)$$

where,

V_r = Reflecting Voltage
V_t = Transmitting Voltage
V_i = Input Voltage
P_r = Reflecting Power
P_t = Transmitting Power
P_i = Input Power

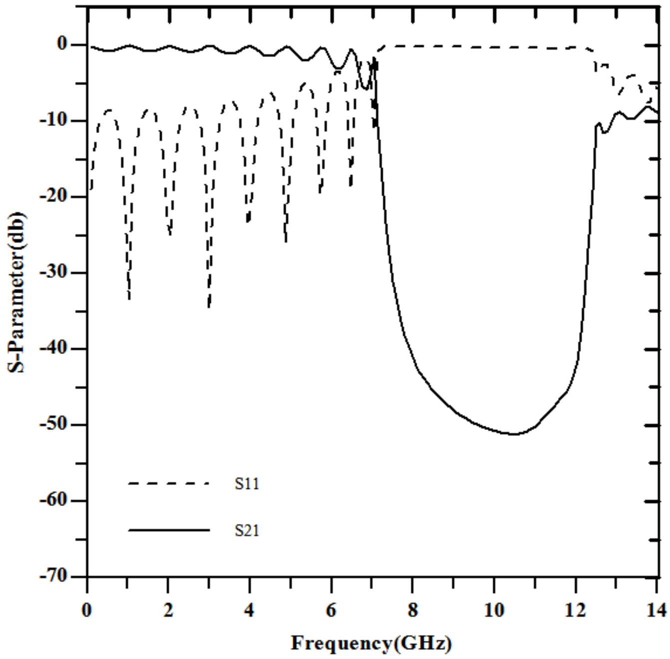

Fig 1.4. S-parameters performances of three lines uniform square-patterned EBG structures. Here dotted line is called the Return loss (S11), and solid line is called the Insertion loss (S21)

1.3. Objective of The Thesis

The main objective of this thesis is to design EBG assisted microstrip transmission lines and filters. EBG assisted transmission lines are investigated to see their improved performance in terms of wider stopband. In case of EBG assisted filter the bandstop property will be utilized in harmonic suppression. EBGSs will be implemented into the conventional lines and filters. The choice of the proper EBG structure is a vital issue to achieve better performance of the designed components for all the conventional designs. Therefore, the first goal is proper selection of EBG/EBG units, which will yield distinct passband and stopband characteristics of the designed frequency. The EBGSs have different forms and their lattice structures are different. The investigations will be confined mainly to circular and square patterned EBG structures. Uniform EBG structures have constraints of filling factor (FF). FF is defined to be the volumetric ratio of one unit cell to the single EBG element. FF controls the width and depth of the stopband [23]. The general concept of increasing the stopband is the enhancement of FF. But after some value of FF the passband transmission suffers from the worst performances. The passband return loss performance is also very poor. To alleviate these problems uniform circular EBGSs with an optimized value of 0.25 [23] and uniform square EBGSs with an optimized value of 0.50 are used.

Then DS-DGSs will be investigated. In the open literature, researchers used uniplanar compact photonic bnadgap structure (UC-EBGS) or DGSs to improve the performance of the filter designs. T. Itoh et al. [24] have proposed UC- EBGS in the ground plane of parallel couple lined BPF and we will use the BPF as our reference filter. Such structures/configurations need careful attention for both top and bottom layers of planar substrates [25, 26]. Attention will be devoted to develop wide bandgap and BPF performance by the perturbed ground plane only. Intensive investigation will be carried out on narrower slot of DS-DGS structures.

The thesis has the following objectives: Modified EBG elements that will provide broadband, distinct passband and stopband characteristics will be designed. The main objectives are as follows.

- Investigate the conventional EBGSs.
- DS-DGS will be investigated.
- Increasing the bandwidth of stopband.
- Modified DS-DGS will be designed to achieve wider stopband.
- Improved performance will be achieved by varying the height of narrower slot of DS-DGS.
- Improved performance will be achieved with the variation of narrower slots.
- Finally an optimized design of DS-DGS will be realized for better performances.

1.4. Thesis Outline

The followings are the outline of the thesis:

- In **chapter 1**, the introduction of the thesis is reported. This chapter explains about the electromagnetic bandgap structures and the DS-defected ground structures and their significance. Their typical S-parameter performance is shown. Finally, objectives of the thesis are briefly discussed.

- In **chapter 2**, a comprehensive literature survey of EBG structures is reported. The investigations of the previous researchers are reported here. Types and application of EBGS and miniaturization of the designs are reported in this chapter.

- In **chapter 3**, firstly, and ideal transmission line with unperturbed ground plane is discussed. Then, conventional EBGSs and their performance are reported here. The 2-D and 1-D structures have been reported and described the reasoning about choosing the 1-D structure instead of 2-D structures. Then similar area of different shaped EBGS, variation of FFs and number of EBGSs are studied here. Finally, performance of DS-DGS and compactness compared to conventional EBGS are observed.

- In **chapter 4**, different parametric studies of a DS- DGS unit have been reported. Then, different types of modified DS- DGS with their S-Parameter performances have been reported in this chapter. Finally, comparing their performances of different designs an improved design has been discussed. Validity of the simulation results with sufficient explanations are reported in this chapter.

- In **chapter 5**, conclusions, fulfilling the goals of thesis work and recommendation for future work have been presented.

Chapter 2

Literature Survey

2.1. Introduction

Microwave engineers are working with the concept of electromagnetic waves interacting with periodic structures. Periodic structures in either closed metallic or open waveguides have been used for many years, for example, in filters and travelling-wave tubes. Planar versions of these can be found in the form of frequency selective surfaces (FSS) and phased array antennas. In the late 1980s a fully 3-D periodic structure, working at microwave frequencies, was realized by Yablonovitch and his co-workers by mechanically drilling holes into a block of the dielectric material [1].

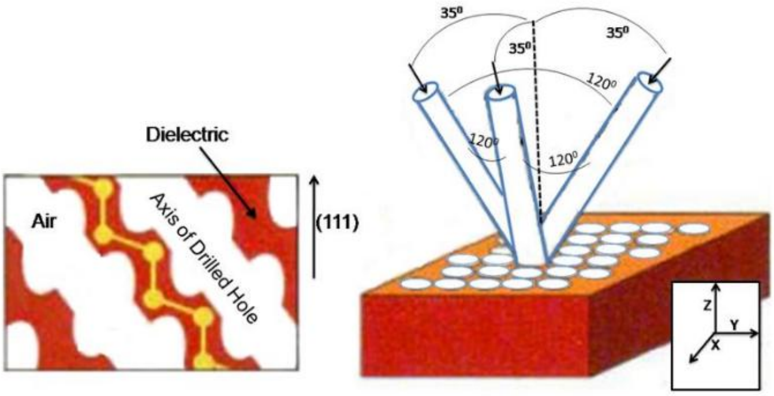

Fig 2.1. First Photonic Crystal by Yablonovitch

This so-called material Yablonovite, prevents the propagation of microwave radiation in any three dimensional spatial direction whereas the material is transparent in its solid form at these wavelengths. These artificially engineered materials are generically known as photonic bandgap (EBG) materials or photonic crystals. Although photonic" refers to light, the principle of bandgap" applies to electromagnetic waves of all wavelengths. Consequently, there is a controversy in the microwave community about the use of the term "Photonic, and the name Electromagnetic bandgap (EBG) material or Electromagnetic crystal [27].

EBG materials are presently one of the most rapidly advancing sectors in the electromagnetic arena. They allow us to manipulate the propagation of electromagnetic waves to an extent that was previously not possible. The rapid advances in both theory and experiment together with substantial technological potential have driven the development of EBG technology. Emphasis is now placed on finding tangible applications combined with detailed modeling. Owing to the tremendous potential of EBGSs there is a plethora of applications in which they can be used [17].

Various works on the recent development of EBGSs have been reported in this chapter. EBG structures are found to play vital roles in enhancing the performance of the microwave components and devices. The stopband characteristic causes the significant improvement in the performance by suppressing surface waves, leakage and spurious transmission [16]. Filling factor (FF) is one of the important controlling factors to yield wider and distinct stopband that should be optimized to maintain a smoother transmission in the passband. In the literature for uniform circular and rectangular patterned EBGSs the optimum filling factors are considered. In case of uniform circular EBG element the optimum FF is considered to 0.25 [23]. But for non-uniform EBG elements, it has been stretched up to 0.45~0.50 [28]. These types of designs are considered as the conventional EBG structure design. Besides, the researchers have worked out on DS-EBGS.

2.2. Types of EBGSs

EBG structures are periodic in nature, which may be realized by drilling, cuffing, and etching on the metal or the dielectric substrates. They may be formed in the ground plane or over the substrate. On the basis of dimensions EBG structures are categorized as one dimensional (1-D), two dimensional (2-D), and three dimensional (3-D) periodic structures that satisfies Bragg's conditions, i.e., inter-cell separation (period) is close to half guided wavelength ($\lambda g/2$). They are capable of forbidding electromagnetic propagation in either all or selected directions [29] [30].

- **3-D EBG Crystals**

In the beginning a 3D EBG was designed only. A successful attempt to obtain 3-D periodic the dielectric structure was made in Iowa State University (ISU) [31]. It was called the woodpile structure as shown in the figure. Three dimensional EBG crystals have periodicity along all the three dimensions and the remarkable feature is that these systems can have complete band gaps, therefore that propagation states are not allowed in any direction [32].

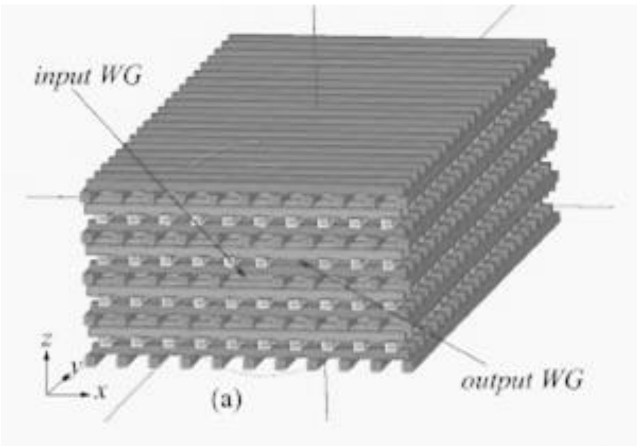

Fig 2.2. Three dimensional EBG Structures [30]

Although, a perfect 3-D EBG structure is required to block all waves in all directions, but then these structures are difficult to fabricate and integrate. From literature, we learned that

2-D EBG could be even more valuable. 2-D EBG structures are easy to fabricate and are capable of maintaining a similar control on the wave propagation in the structure as the 3-D structure.

- **2-D EBG Crystals**

These crystals have periodicity in two dimensions and are homogeneous along the third direction, or we can say that, all variations happen in the two dimensions, whereas everything is constant along the third dimension, thereby propagation is allowed along one axis of the crystal [30]. These 2-D EBG structures have substantial advantages in terms of compactness, stability, and fabrication, which make them more attractive for microwave devices [32].

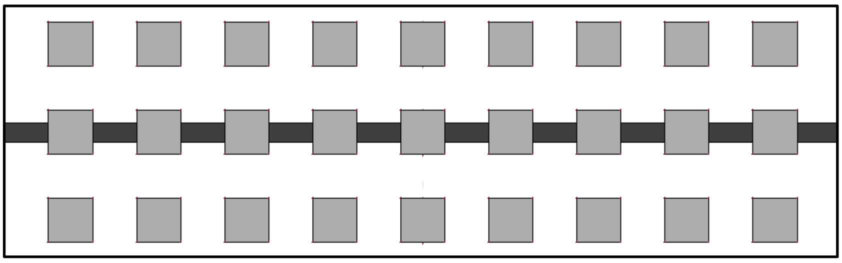

Fig 2.3. Two dimensional EBG structures.

One of the greatest advances in the development of these 2-D EBG structures in microwave range has been their implementation in microstrip technology.

- **1-D EBG Crystals**

One dimensional EBG structures can also be implemented in microstrip technology. 1-D EBG structures have periodicity of two different media along one direction only. These basic crystals exhibit three important phenomena: photonic band gaps, localized modes, and surface states. However, as the index contrast is only along one direction, the band gaps and bound states are limited to that direction. Nevertheless, these simple structures show most of the features of 2-D and 3-D EBG crystals [33].

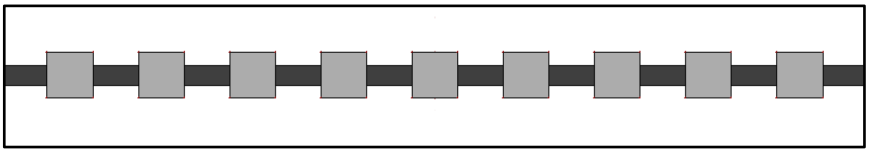

Fig 2.4. One dimensional EBG structure

2.3. Application of EBGS

Now a day's microwave communication system requires compact size, high performance and low cost devices. To fulfill the requirement and to enhance performance some new structures like EBGSs exist on the communication system. In recent days, many researchers give their attention to EBGSs due to their unique properties. A summary of their works in this section are briefly discussed in this section.

a. Power amplifiers

EBGS can produces the desired stopbands and passbands by creating a spatially periodic variation of the effective the dielectric constant of the line. Broad-band operation of power amplifiers requires harmonic filtering and tuning that is typically difficult to realize. The wide stopband characteristic of microstrip on EBG ground plane can be used as broad-band harmonic tuner for power amplifiers to increase power added efficiency [34].

b. Resonators

Resonators based on EBG technology have been proposed as an alternative to current technologies [35-38]. Resonator structures can be fabricated on different laminates by using inexpensive standard printed circuit board (PCB) processing techniques and can be used in commercial products. Tim Eular and John Papapolymeror proposed a micro- machined resonator at 45 GHz based on defect induced EBG laminate with high quality factor and low losses [35].

c. Filters

Filters based on EBG structures have also been demonstrated. For example, Rumsey et al. [39] presented a lowpass filter with a wide high frequency rejection bandwidth using cascaded sections of EBG structures with different lattice periods. Horii et al. [40] presented a microstrip patch antenna with EBG ground plane to suppress radiation at harmonic frequencies while Deal et al. [41] used the same structure to reduce power lost to surface waves. Chang et al. demonstrated EBG resonators for microstrip line and CPWs [42].

Some other researchers also designed high quality factor filters [35, 36], with high isolation [37] and low insertion losses [37, 38] with wide bandwidth. The concept of EBGs has been utilized to develop the devices of high isolation with high quality factor that can integrate monolithically with other components. According to the demands, Chappel and his co-workers designed 2, 3 and 6 pole filters using mettalothe dielectric EBG lattice. Chappel also designed a wide bandgap structure using the high-k ceramics, which was embedded into a polymer to create an EBG substrate. J. C Vardaxoglu et. al. also proposed a tunable wide bandgap using mettalo-the dielectric EBGs [43]. Hell and his team proposed a reconfigurable EBG cavity resonator with low insertion losses [44]. The use of EBG circuits for filter applications [23, 45-49] in microwave technology has been proposed in different ways. Vesna Radistic designed the EBG by etching a 2-D structure of holes in the ground plane of the microstrip circuit [36].

d. Spurious-Free Microstrip Filters

The previous structure can be exploited to suppress spurious passband always present in conventional microstrip filters [49-50]. The sharp cutoff can be exploited to improve the roll-off of a lowpass filter [50]; meanwhile, the slow wave effect reduces the resonator length of the filter integrated with UC-EBG ground plane [49].

e. Harmonic Tuning in Power Amplifier

Harmonic tuning in power amplifier using the UC-EBG has been demonstrated [51]. An S-band class AB power amplifier integrated with UC-EBG microstrip has been investigated [34]. Improved performance with harmonics suppression had achieved.

f. Aperture-Coupled Patch Antenna on UC-EBG Substrate

Microstrip patch antennas are extensively used in communication systems for their low profile, low cost and easy fabrication [39]. Patch antennas are usually built on low permittivity substrates for optimum performance since surface waves are excited on a high the dielectric constant substrate. On the contrary, MIC and MMIC are usually built on high the dielectric constant substrates to reduce the dimensions. To achieve a high degree of integration for both circuits and antenna is desirable to realize planar antennas with good performance on high the dielectric substrates. The complete stopband provided by the UC-EBG structure can be employed to reduce surface wave losses of patch antennas on high the dielectric constant substrate [52 - 54].

g. Low Pass Filter (LPF)

To produce compact designs using the "Uniplanar Compact EBG Structures" where, the slow wave effect is produced by a distributed LC two-dimensional structure, which allows a considerable size reduction in the circuit. A spurious-free bandpass filter and high-performance, low pass filter using a coupled microstrip, was proposed by Fei-Ran Yang and his group [49].

In this case, the UC-EBG structure shown in the figure is used in the ground plane to improve the performance of conventional LPF [49]. A small portion of the 50-ohm feed line is placed on the perforated ground plane (UC-EBG plane), the remaining being on the solid ground plane. Duroid substrate is used with ε_r = 10.2 and the thickness of the substrate is 25 mils. The width of the 50-ohm microstrip is 24 mils. The simulation result shows the wider stopband above 6 GHz and S_{21} is found to be under –30 dB for a wide frequency range. Within the stopband range, the return loss is found to be about 0 dB, indicating very little radiation loss which also verifies the EBG property. A stepped-impedance LPF with seven reactive elements has been chosen [55].

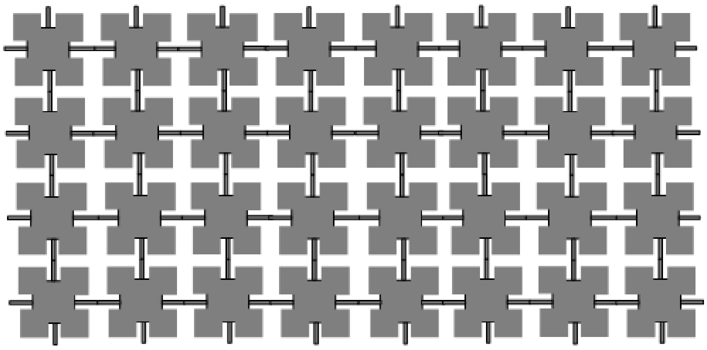

Fig 2.5. UC-EBG structure

h. Bandpass Filters (BPF)

Conventional parallel-coupled bandpass filters (BPF) need extra filters to suppress the spurious transmission that results in the increase of insertion loss. It is reported [56] that the use of extra filters can be avoided by just applying EBG to obtain a compact microstrip BPF with intrinsic spurious rejection. The well-matched microstrip on the UC-EBG ground plane is suited as a low-loss transmission line. The generated spurious passbands at higher harmonics can be suppressed with the aid of EBGS as it provides a wide and deep stopband. The physical length of the filter circuit is reduced as well due to the slow-wave effect of the UC-EBG structure. The figure shows the schematic of a microstrip BPF on the UC-EBG ground.

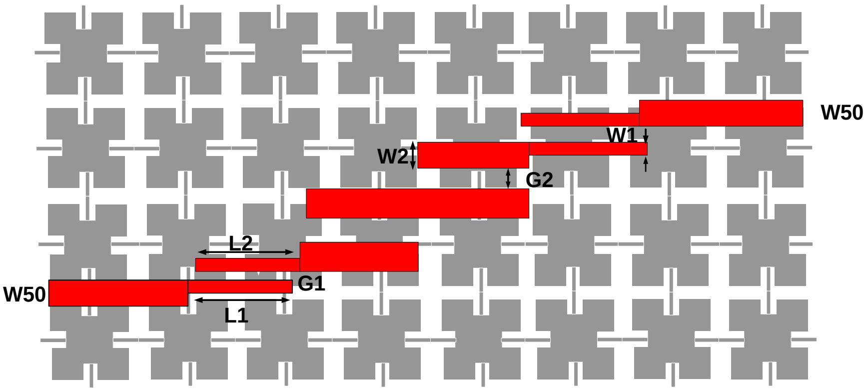

Fig 2.6. Schematic diagram of a BPF over UC-EBG

The reference [55] narrates the standard design procedures of the parallel-coupled BPF. The requirements are [56]:

At the frequency of 12 GHz and 17 GHz, transmission coefficient of a conventional BPF are seen to be –10 dB and -5 dB respectively. On the other hand, the UC-EBG assisted filter provides the spurious suppression of 30-40 dB. Though the length of the microstrip resonator has been scaled accordingly to the slow-wave factor, the coupling gap remains same, which results in the increased fractional bandwidth (21.6 %) at 6 GHz center frequency. Like conventional BPF the coupling co-efficiency can be optimized to improve the bandpass characteristics of the EBG assisted BPF. Including the effect of two SMA connectors, the minimum insertion loss of the EBG assisted filter is found to be 1.9 dB at 6.39 GHz.

Loptegi and his researchers also designed different bandpass filters using defect ground structures [57]. Ducain Nesic proposed a EBG microstrip slow wave structure. This proposed structure exhibits slow wave and low pass characteristics. It was fabricated by using a modified microstrip line, without etching the ground plane [58-60].

2.4. Miniaturization

Miniaturization of microwave devices and antennas has become increasingly important in recent years. Modern wireless communication systems require small microwave elements that are relevant to high-level integration into compact lightweight systems. Miniaturization can be achieved by several techniques. Roger and his co-workers designed a magnetic conductor and to reduce its size and cost. In order to do that they integrated some capacitance of the FSS without resorting to the second layer of overlapping patches [61]. By increasing the capacitor and inductor in Sivenpiper High Impedance Surface, size of the EBG cell was reduced [62]. Feresidis et. al. introduced the concept of closely coupled metallo the dielectric electromagnetic band-gap structure, and designed 2-D double layer dipole arrays. These arrays are closely packed [63]. It is well known that at certain frequencies outside the band gap, periodic structures support waves, commonly termed as slow waves, with reduced phase velocity and guided wavelength with respect to the wave propagating in a comparable homogeneous medium. This property can be exploited for the miniaturization of microwave elements, such as the triple array elements [64]. An approach to this is to examine elements with periodic loading. Multiple-order periodic loading of basic elements possesses a good degree of flexibility in the design [64, 65].

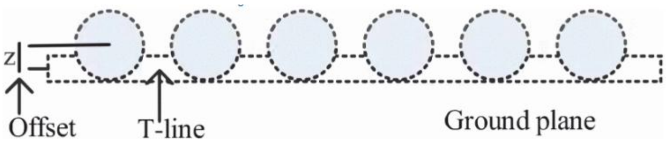

Fig 2.7. Offset in uniform EBGS assisted T-line [67]

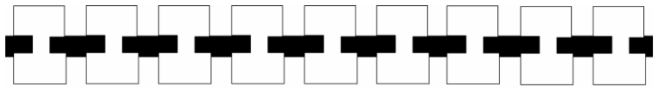

Fig 2.8. EBGS assisted microstrip T-line having DS-EBGS with rectangular bigger slots [68]

Fractal-type structures are subsequently produced using second-order loading. This can also be used for multiband AMC designs [66]. Another way of increasing the length of the loading stubs without increase the unit cell and at the same time to increasing the capacitive coupling between successive elements is the inter-digital topology. The loadings of successive dipoles are shifted so that they can extend to the full length allowed by the array geometry.

Chapter 3

Conventional EBG Assisted T-Line

3.1. Introduction

Electromagnetic Bandgap (EBG) technology represents a major breakthrough with respect to the current planar approaches, mainly due to their ability to guide and efficiently control electromagnetic waves. As the frequency increases, a planar structure that integrates the antenna, mixers, local oscillator, and all peripheral circuitry onto one single substrate becomes an attractive option.

Planar EBG's are of particular interest at microwave frequencies due to ease of fabrication. These EBG's are usually periodic in one and two dimensions. Planar EBG structures consist of uniformly distributed periodic metallic patterns on one side of a dielectric slab. They exhibit some interesting features such as distinctive passband and stopband, slow wave effects, low attenuation in the passband and suppression of surface waves when serving as the ground of planar microstrip circuit. Several Planar EBG configurations have been reported in the literature like uni-planar designs without vertical vias, one and two-dimensional EBG transmission line design etc. in which they used EBG basis points with different geometries, and shapes like circular shape, square, hexagonal, fork shape, plus sign and many more. In some planar devices, they create defects by creating a discontinuity in a periodic pattern. For example in a planar circular defect induced EBG structure with lattice, they remove some circles or change their size for creating some discontinuity. Some of these types of EBG structures are shown in the figure.

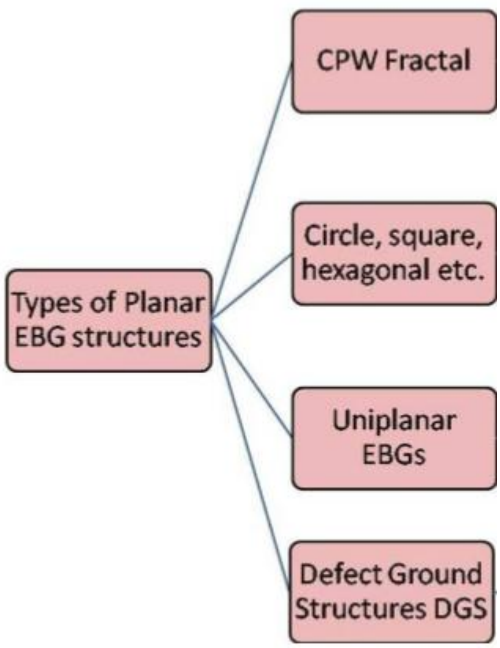

Fig 3.1. Classification of Planar EBG Structures

3.2. Microstrip Structure

The general structure of a microstrip is illustrated in the figure. A microstrip line with a width W and a thickness t is on the top of a dielectric substrate that has a relative the dielectric constant ϵ_r and a thickness h, and the bottom of the substrate is a ground (conducting) plane.

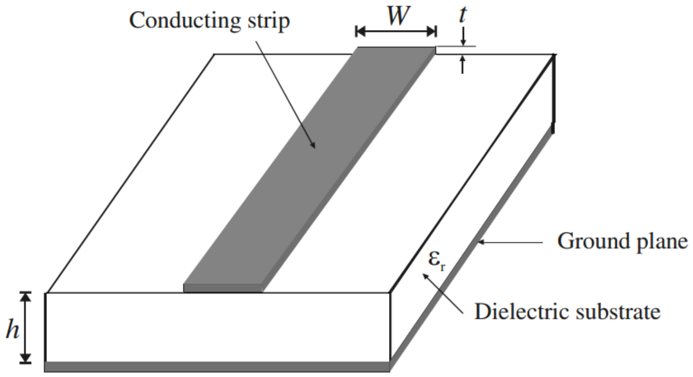

Fig 3.2. General microstrip structure.

3.3. Uniform EBG (UEBG) Configurations Applied To Microstrip Lines

In modern microwave devices, microstrip transmission lines are most common. Therefore, in the following sections, the investigation is concentrated into only on EBG assisted microstrip transmission line. To derive the characteristic performance of EBG assisted lines it is more logical to use scattering parameters (S-parameters) instead of showing K-β diagram. S-parameters have universally accepted the format of device characterizations. Moreover, commercially available software tool Zealand IE3D will be used to design and to extract S-parameters for all designs due to the flexibility of Zealand IE3D. Zealand IE3D is a method of moment (MOM) based full-wave analysis tool, hence very accurate.

The perturbation in the ground plane of any microstrip transmission line in the form of EBGS creates stopband that is useful for suppression of surface waves, leakage, and spurious transmission and to improve the performance of antennas, filter, and other microwave devices and components. The stopband characteristic is highly influenced by the shape, size and the period of the EBGSs located on the ground plane. Therefore, it is useful to see the performance of the standard 50-ohm microstrip transmission line on EBGSs. The lines will be investigated to see the performance of three rows of uniform EBG structure as [43]. In this section, uniform circular and square patterned EBGS will be investigated. It is well known that the EM field is highly concentrated under the microstrip line. Under this consideration, one dimensional (1-D) uniform EBGS (one line) will be investigated and compared the result with 2-D structure (three lines). Finally, 1-D EBGS will be used as two structures yield similar performances.

3.4. Design of Microstrip Transmission Line over Uniform EBGS

In EBG engineering, it is a conventional rule to use Bragg's condition [60] to calculate the central stopband frequency provided by EBGSs. Under this condition, inter-cell separation or period is approximately equal to the half wavelength of the stopband central frequency. From the inter-cell separation, the size of the EBG element is calculated on the basis of the Filling factor (FF). With the inclusion of EBGSs the dispersion characteristics of a transmission line change. At first, a microstrip transmission line with the unperturbed ground plane is designed that does not provide any stopband characteristics. Then, the period of the EBG elements is determined for the design by using PCAAD and the designing equations.

- **Determination of Transmission line width**

The geometry of the design is patterned under 50 ohm transmission line are designed by using "Taconic Substrate" in which relative the dielectric constant $\varepsilon_r = 2.45$, Thickness, h=31mil or 0.787mm. Using Personal Computer Aided Antenna Design 5.0 (PCAAD) software the values of transmission line width, w = 0.2263 cm and effective the dielectric constant, $\varepsilon_{eff} = 2.068$ has been found.

- **Explanation of the designing equation to determine the inter-element spacing (period)**

To determine the period we need to follow the equations. We know that, wavelength,

$$\lambda_0 = \frac{300\ (mm)}{f_c\ (GHz)} \tag{3.1}$$

where, f_c = Centre frequency.

$$\lambda_g = \frac{\lambda_0}{\sqrt{\varepsilon_{eff}}} \tag{3.2}$$

From the Bragg's condition[60] we have the equation of the period as,

$$a = \frac{\lambda_g}{2} \tag{3.3}$$

Filling factor, FF $= \frac{r}{a}$ (3.4)

where, r = radius of circular EBGS, a= inter-element spacing.

The center frequency of the stopband is calculated approximately with the following expression:

$$\beta a = \pi \tag{3.5}$$

where β is the wave number in the dielectric slab and is defined by the expression:

$$\beta = \frac{2\pi f_0}{c}\sqrt{\varepsilon_{eff}} \tag{3.6}$$

where,

f_0= the center frequency of the stopband

ε_{eff} = the effective relative permittivity of the the dielectric slab

c = the speed of light in free space

For example, if $f_c = 10\ GHz$,

$$\lambda_0 = \frac{300}{10} = 30\ mm$$

$$\lambda_g = \frac{\lambda_0}{\sqrt{\varepsilon_{eff}}} = \frac{30}{2.068} = 20.86\ mm$$

Now,

$$a = \frac{\lambda_g}{2} = \frac{20.86}{2} = 10.43\ mm$$

- **Size Calculation**

Filling factor (FF) = r/a for circular EBGS. FF has optimized value of 0.25 [28]. Therefore, r= a*FF. In the present case, r = 10.43*0.25 = 2.6 mm. This is the value of radius of the circular EBGS

- **Standard 50-ohm transmission line**

In this case, the ground plane is fully unperturbed. A standard 50 ohm line is realized on Taconic substrate having the dielectric constant of 2.45 and height of 31 mils.

Fig 3.3. Design of a standard 50 Ω transmission line

The S-parameters of the designs have been investigated to conceive the idea of 1-D EBGSs in lieu of 2-D EBGSs, optimized FF and the influence of the number of EBGSs on the dispersion characteristics of the microstrip transmission line. The Taconic substrate is used in the simulation for the ideal and uniform structured EBGSs. The simulated S-parameters performances of an ideal transmission line are shown in the figure. The insertion loss is approximately zero dB throughout the whole frequency range from 0 to 14 GHz.

It can be seen from the graph that the signal is transmitting between two ports of the transmission line with negligible loss. Therefore within the whole range of frequencies, there is no stopband. The return loss performance of the ideal microstrip line over the whole frequency range is also excellent and >10 dB. Obviously, the S-parameters performance shown in figure characterizes an ideal transmission line.

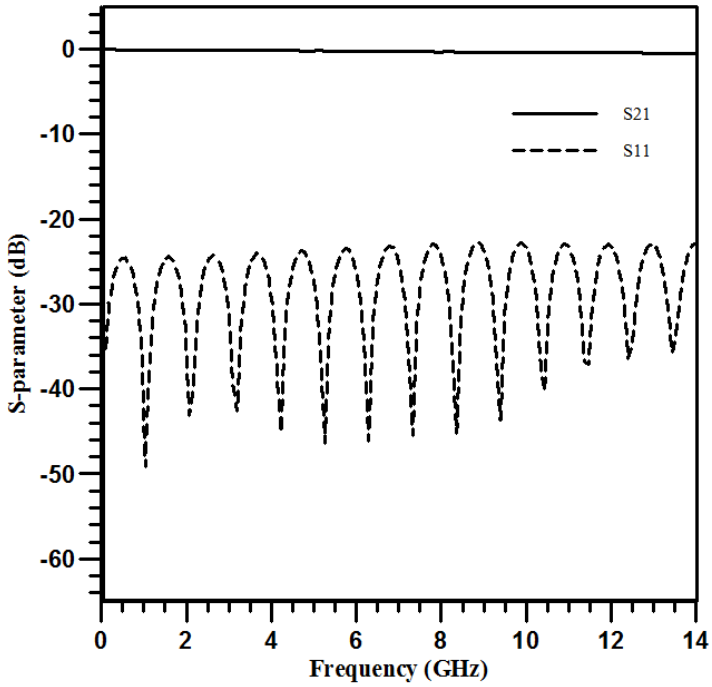

Fig 3.4. IE3D simulated S-parameters versus frequency of an ideal 50-ohm transmission line. The substrate is Taconic having the height of 31 mils and the dielectric constant is 2.45

- **Designs of EBG assisted T-line with Uniform Circular EBGSs**

The following different microstrip transmission lines have ground planes with different EBGSs. All the EBGSs are designed at the stopband central frequency of 10 GHz.

- **2-D uniform circular in the ground plane:**

Here three-line circular EBGS has designed. This design gives the idea of the optimum value of FF to be 0.25. The geometry of a three rows (2-D) uniform hole patterned EBGSs in the ground plane of a 50 ohm transmission line is shown in the figure.

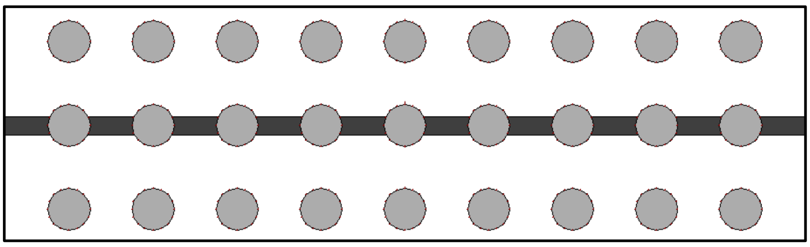

Fig 3.5. Geometry of a 50-ohm microstrip transmission line where 2-D (three-line) uniform circular EBGSs are etched in the ground plane.

At first, small uniform and circular holes have been introduced in the ground plane to observe their effects on the performance of a standard 50 ohm transmission line. The radius of the uniform circular EBGSs are 2.6075 mm and the period is 10.43 mm. The S-parameters performance is shown in figure. It can be seen from the figure that this design provides wider passband and deeper stopband. The 10 dB return loss bandwidth is found to be 6.35 GHz; the 20 dB rejection bandwidth is 4.35 GHz. The ripple height along the passband is negligible. But around cut-off frequencies, ripples are observed. The center frequency is found to be shifted around 10.06 GHz resulting in 1% frequency deviations from the design frequency. The maximum value of isolation is found to be 61.42 dB.

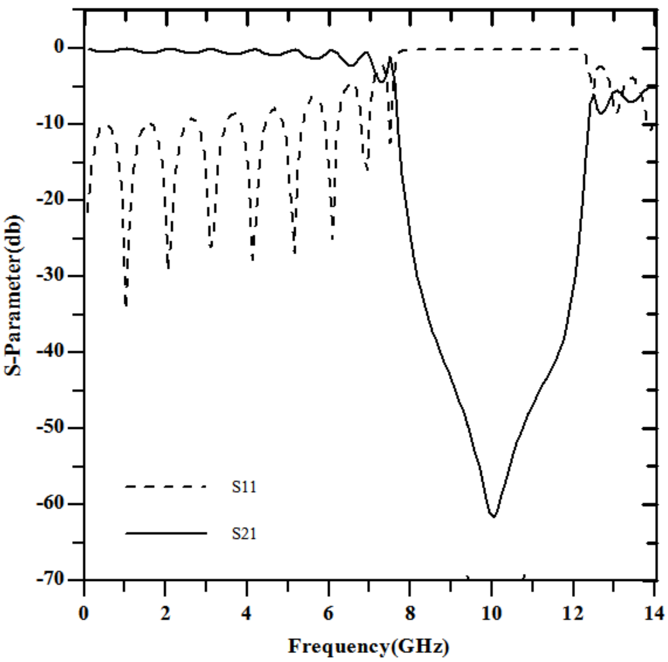

Fig 3.6. Simulated S-parameter performances of a standard 50- ohm transmission line perturbed by 2-D (three lines) uniform circular EBGSs in the ground plane. The substrate is Taconic having the height of 31 mils and the dielectric constant of 2.45. The uniform circular EBGSs are of 2.6075 mm and the period is 10.43 mm (FF=0.25).

- **1-D uniform circular EBGSs with FF of 0.25:**

This design will yield the performance to consider 1-D EBGSs that replace 2-D EBGSs. The geometry of the 1-D uniform hole patterned EBGSs is shown in Figure 4.7. In this design, only one row of EBG elements is etched in the ground plane just under the 50 ohm transmission line.

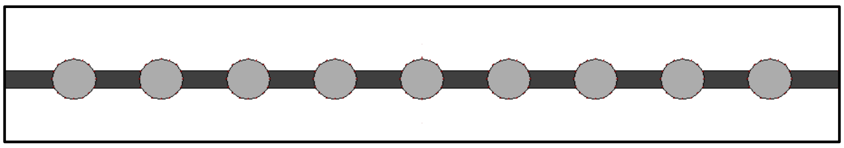

Fig 3.7. Geometry of a standard 50-ohm transmission line with 1-D uniform circular EBGSs etched in the ground plane.

It is mentioned that 0.25 is the optimum FF for Taconic with the dielectric constant of 2.45 and height of 31 mils. Based on this value a microstrip transmission line with 1-D uniform circular EBGSs has also been investigated. The simulation result is shown in the figure.

From the figure, it can be seen that return loss performance, stopband characteristics and ripple height for this design are similar to 2-D design. A negligible difference in the value of maximum isolation is observed. In the case of three rows of uniform circular EBGSs, the maximum isolation is found to be approximately 61.6 dB. On the other hand, one row of uniform circular EBGS provides approximately 61.46 dB.

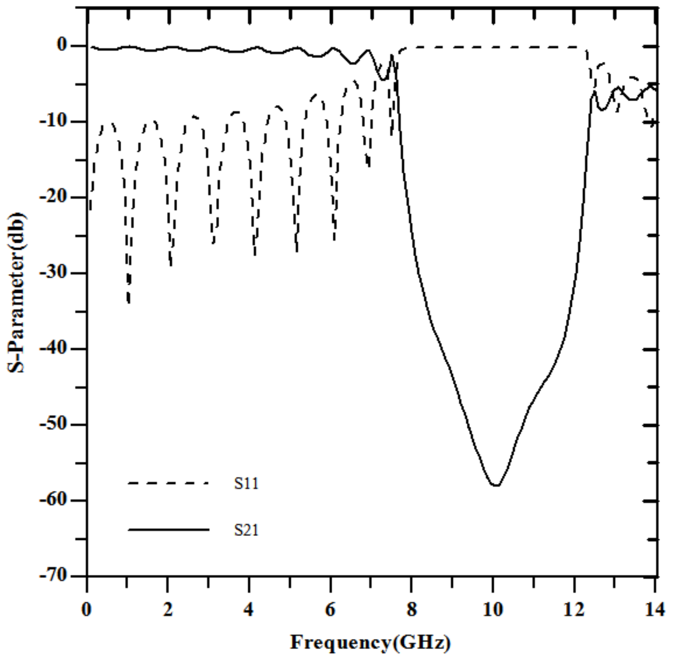

Fig 3.8. Simulated S-parameter performances of a standard 50 ohm transmission line perturbed by 1-D (one line) uniform circular EBGSs in the ground plane.

From these figures (Figure 3.6 and 3.8) it is very clear that 1-D EBGSs and 2-D EBGSs provide very similar performances.

- **Designs of Uniform Square Patterned EBGSs**

Uniform square patterned EBGSs will also be designed. Here three rows and one row EBGSs will be designed and their performances will be compared. It will be useful to replace three rows EBGSs by 1-D EBGSs. On the basis of the availability of the materials for the fabrications Taconic substrate with ε_r = 2.45 and height (h) = 31 mils is used in the simulation.

- **2-D Uniform Square Patterned EBGSs**

The conventional uniform square patterned EBGSs are shown in the figure. Three lines of total 27 EBG elements are etched under the standard 50-ohm transmission line. The FF is taken to be 0.5.

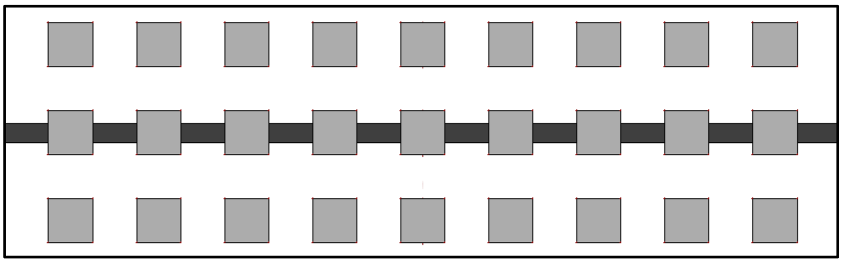

Fig 3.9. 2-D (three lines) of square patterned EBGSs under standard 50 ohm transmission line. Substrates: ε_r = 2.45 and height (h) = 31 mils and tan δ = 0.002. The inter-element spacing, a= 10.43 mm, element width and length, b = 5.215 mm.

The S-parameters performances of uniform square patterned EBGSs have also been analyzed. The simulated and measured S-parameters performances of three lines (2-D) uniform square patterned EBGSs are shown in the figure.

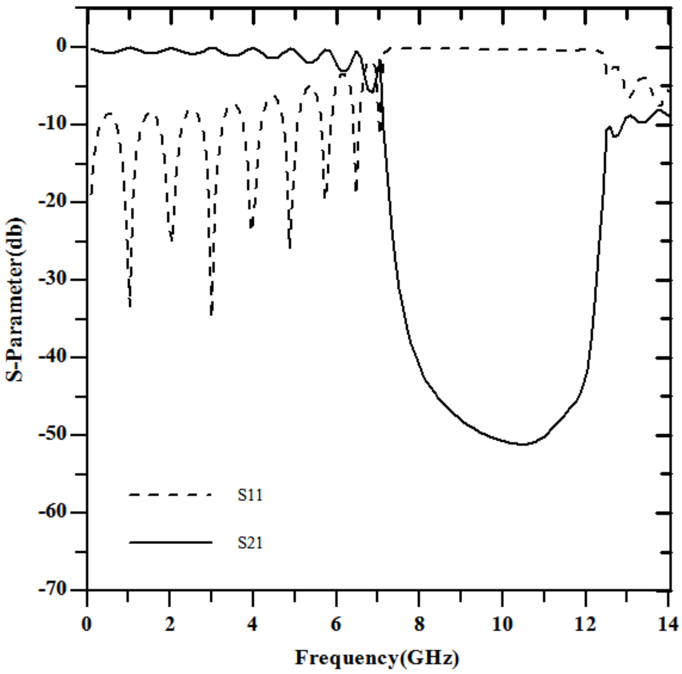

Fig 3.10. S-parameters performances of three lines uniform square-patterned EBG structures. The substrate is Taconic having the dielectric constant of 2.45 and height of 31 mils. The inter-element spacing is 10.43 mm and FF is 0.5.

- **1-D Square patterned EBGSs**

The geometry of 1-D (one line) circular patterned EBGSs is shown in the figure. Here only 9 EBG elements are etched in the ground plane.

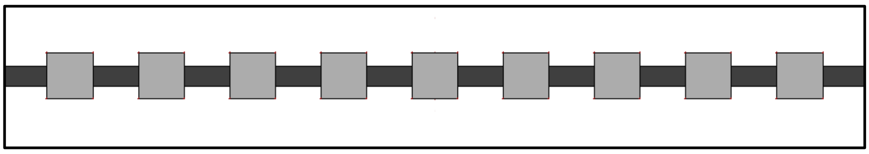

Fig 3.11. 1-D square patterned periodic structures under the standard 50-ohm transmission line. The substrate is Taconic having the dielectric constant of 2.45 and height of 31 mils. The inter-element spacing, a= 10.43 mm, element width and length, b = 5.215 mm.

It is mentioned that 0.5 is the optimum FF for Taconic with the dielectric constant of 2.45 and height of 31 mils. Based on this value a microstrip transmission line with 1-D uniform rectangular EBGSs has also been investigated. The simulation result is shown in the figure.

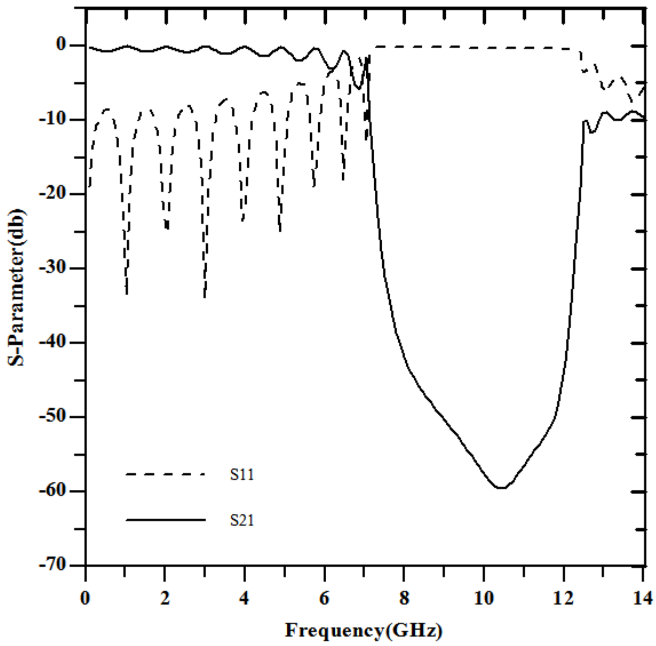

Fig 3.12. Simulated S-parameter performances of a standard 50 ohm transmission line perturbed by 1-D (one line) uniform rectangular EBGSs in the ground plane.

From the figure, it can be seen that return loss performance, stopband characteristics and ripple height for this design are similar to 2-D design. A small difference in the value of maximum isolation is observed. In the case of three rows of uniform rectangular EBGSs, the maximum isolation is found to be approximately 51.1 dB. On the other hand, one row of uniform rectangular EBGS provides approximately 59.8 dB.

3.5. Designs of Uniform Circular EBGSs using the same area of different EBGS

Some 1-d uniform circular, rectangular and patterned EBGSs with same areas will be designed. In the design, we take the radius of circular EBGs is r=2.6075 mm. So, for taking the similar area of different types of EBGS, the arm of a rectangular EBGS will be calculated as well as EBGS.

Here, the area of a circular EBGS= πr^2 (3.7)

Area of rectangular EBGS = b^2 (3.8)

So, $b = \sqrt{\pi r^2}$ = $\sqrt{\pi \times 2.6075^2}$ = 4.6216 mm

<table>
<tr><th>Figure</th><th>Characteristics</th></tr>
<tr><td>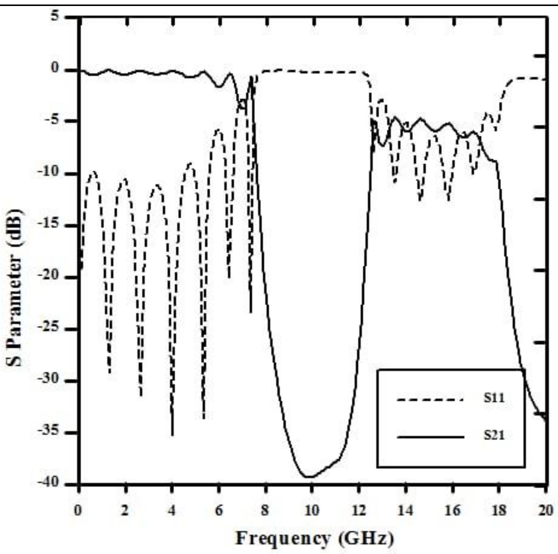
</td><td>Uniform Circular EBGSs
10 dB Return Loss BW= 3.6 GHz
20 dB Rejection Loss BW= 2.1 GHz
Passband Ripple Height= 6 dB</td></tr>
<tr><td>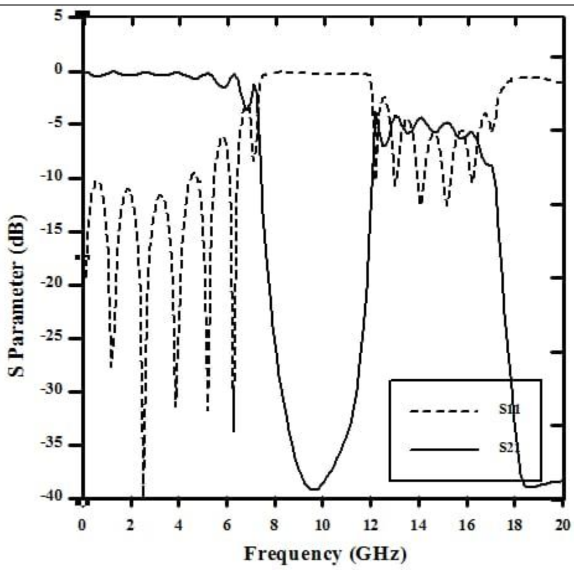
</td><td>Uniform Rectangular EBGSs
10 dB Return Loss BW= 3.5 GHz
20 dB Rejection Loss BW= 2.2 GHz
Passband Ripple Height= 6 dB</td></tr>
</table>

Fig 3.13. Simulated S-parameter performances of 1-D (one line) uniform EBGSs with circular and rectangular EBGSs of same areas.

These designs are done with the circular and rectangular EBGSs of same areas. From this table we could conclude that size does not matter for a different EBGSs pattern of same areas.

3.6. Designs of Uniform Circular EBGSs using different filling factor

Some 1-D uniform circular patterned EBGSs will be designed. Here circular EBGSs with different filling factor will be designed and their performances will be compared. On the basis of the availability of the materials for the fabrications Taconic substrate with ε_r = 2.45 and height (h) = 31 mils is used in the simulation has shown in the figure.

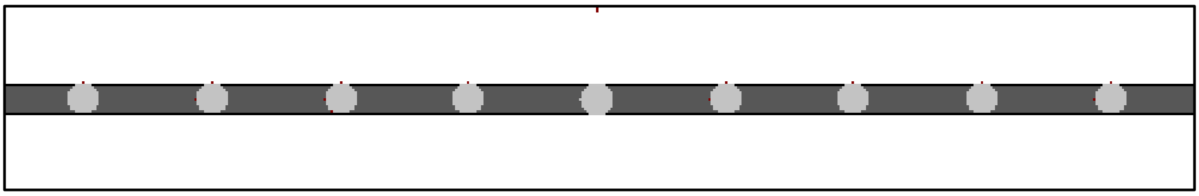

(a)

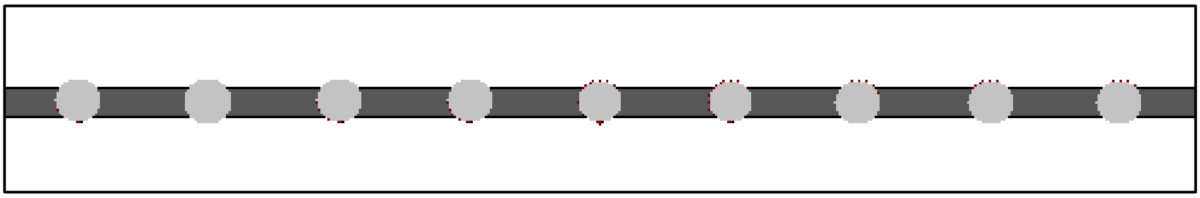

(b)

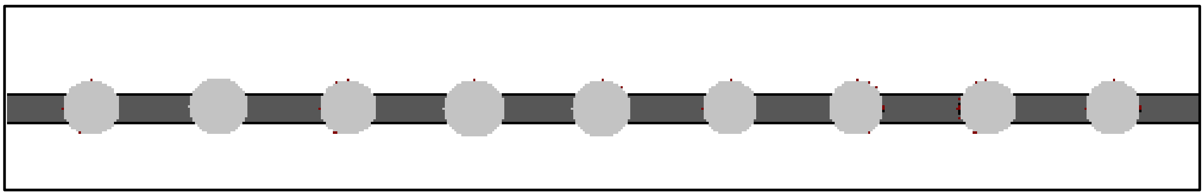

(c)

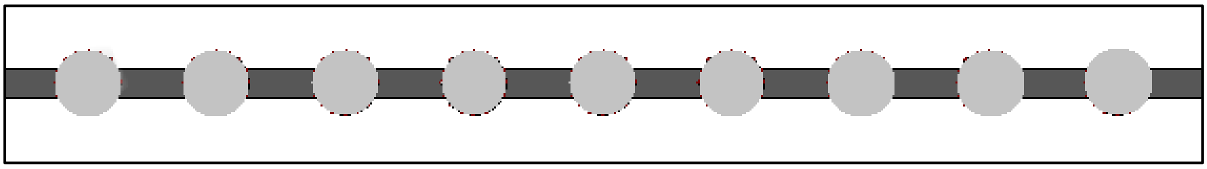

(d)

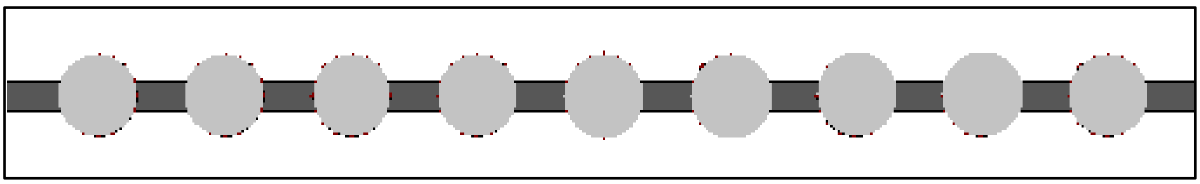

(e)

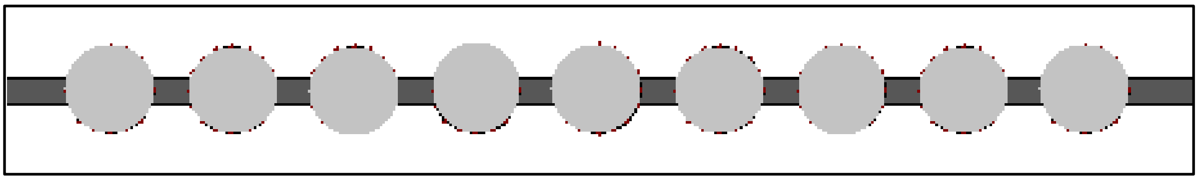

(f)

Fig 3.14. Geometry of a standard 50-ohm transmission line with 1-D uniform circular EBGSs etched in the ground plane with (a) 0.1, (b) 0.15, (c) 0.2, (d) 0.25, (e) 0.3, (f) 0.35 filling factor. The inter-element spacing, a= 10.43 mm.

- **Simulation Results of Uniform Circular EBGSs using different filling factor**

The S-parameters performances of uniform circular patterned EBGSs using different filling factor have also been analyzed. The simulated and measured S-parameters performances of three lines (2-D) uniform patterned EBGSs are shown in Figure.

(a)	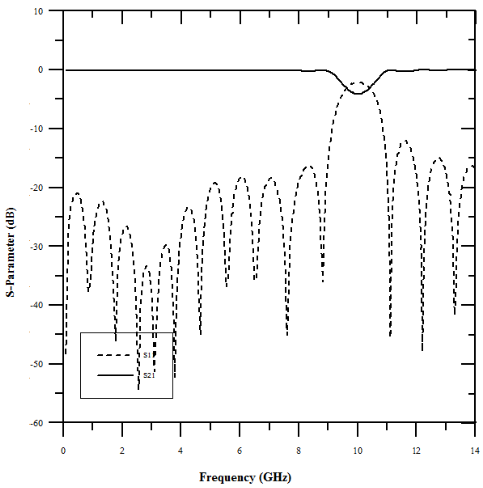	10 dB Return Loss BW= 2.1 GHz 20 dB Rejection Loss BW= 0 GHz Passband Ripple Height= 0 dB
(b)	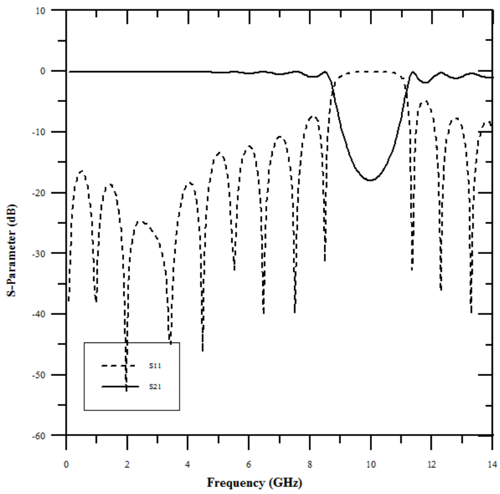	10 dB Return Loss BW= 3.4 GHz 20 dB Rejection Loss BW= 0 GHz Passband Ripple Height= 1 dB

(c)	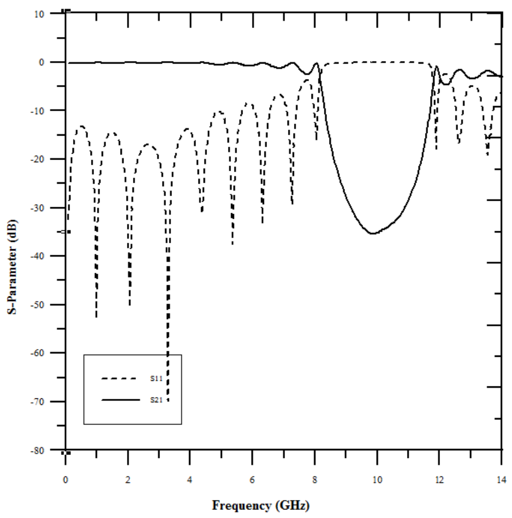	10 dB Return Loss BW= 3.8 GHz 20 dB Rejection Loss BW= 2.8 GHz Passband Ripple Height= 2 dB
(d)	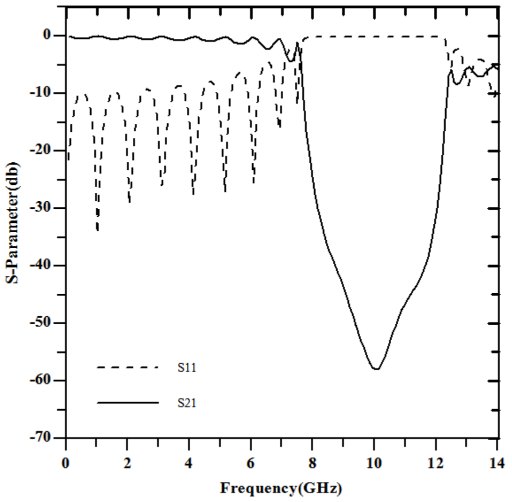	10 dB Return Loss BW= 4.7 GHz 20 dB Rejection Loss BW= 5.2 GHz Passband Ripple Height= 4 dB
(e)	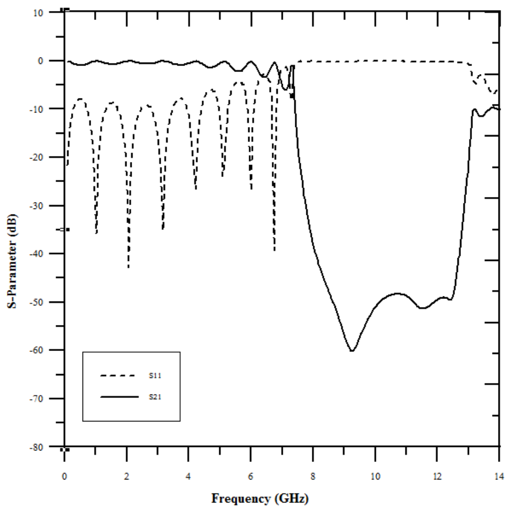	10 dB Return Loss BW= 7.5 GHz 20 dB Rejection Loss BW= 5.8 GHz Passband Ripple Height= 6 dB

(f)	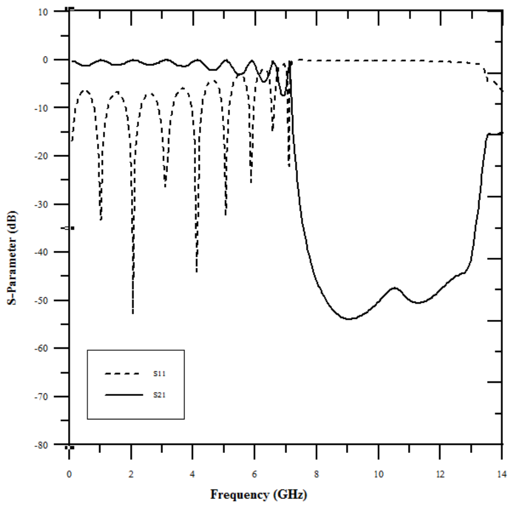	10 dB Return Loss BW= 8 GHz 20 dB Rejection Loss BW= 6.4 Ghz Passband Ripple Height= 7 dB

Fig 3.15. Simulated S-parameter performances of 1-D (one line) uniform rectangular EBGSs with 0.1, 0.15, 0.2, 0.25, 0.3, 0.35 filling factor in the ground plane.

3.7. Designs of Uniform Circular EBGSs using different EBG number

Here Uniform circular DGS has been designed with a different number over the transmission line to test the improvement of the filter. Here it has been shown that the range of EBGS numbers that will give better simulation result of good insertion and return loss.

	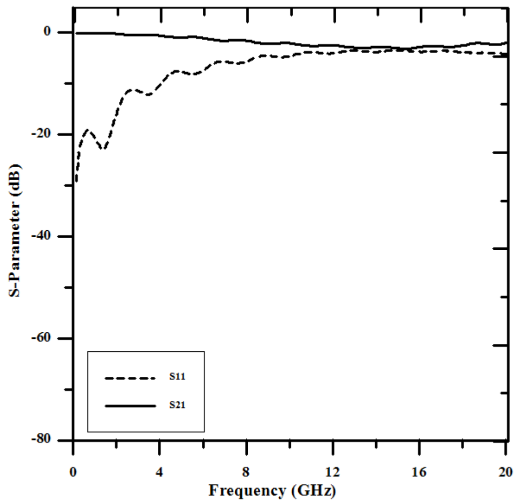

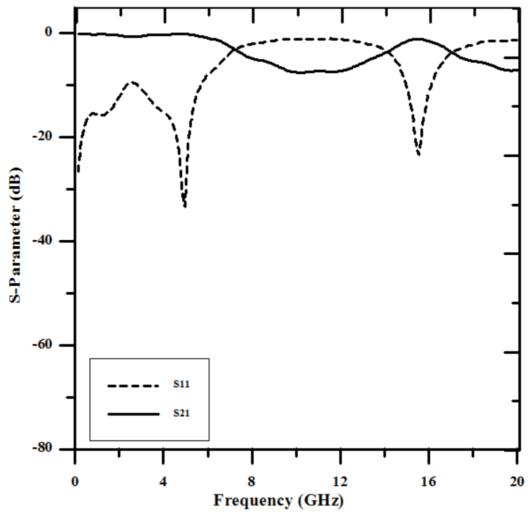
0
-20
-40
-60
-80
S-Parameter (dB)
0 4 8 12 16 20
Frequency (GHz)
S11
S21

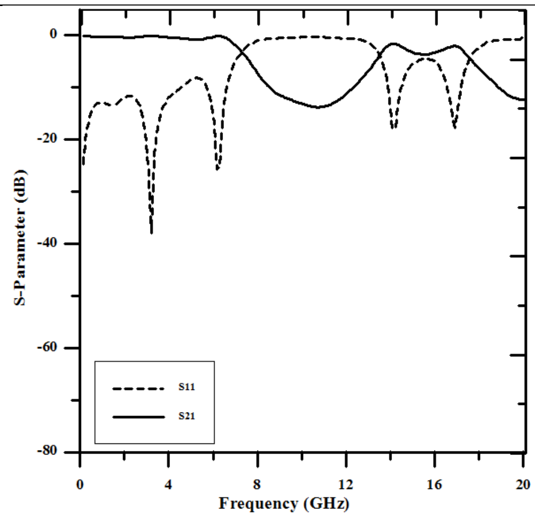
0
-20
-40
-60
-80
S-Parameter (dB)
0 4 8 12 16 20
Frequency (GHz)
S11
S21

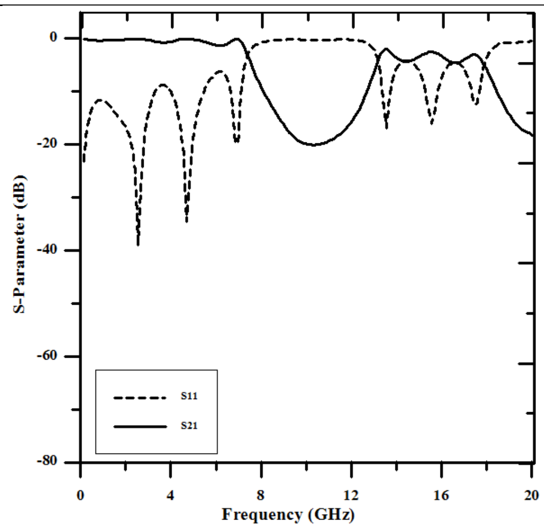
0
-20
-40
-60
-80
S-Parameter (dB)
0 4 8 12 16 20
Frequency (GHz)
S11
S21

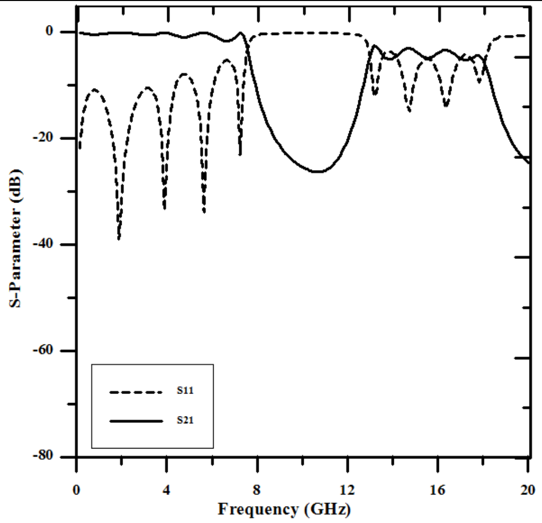
S-Parameter (dB)
Frequency (GHz)
0
-20
-40
-60
-80
0
4
8
12
16
20
S11
S21

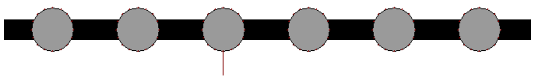

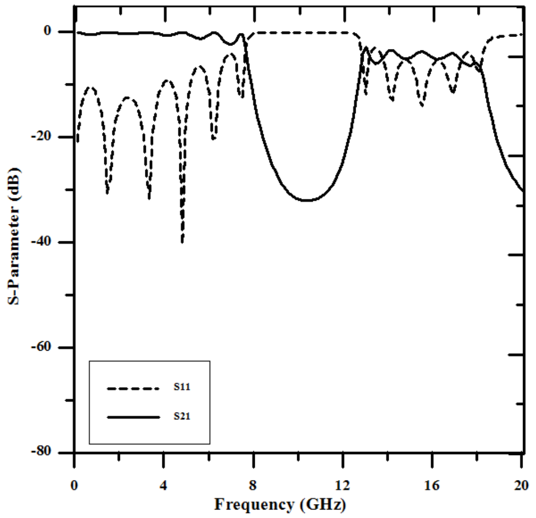
S-Parameter (dB)
Frequency (GHz)
0
-20
-40
-60
-80
0
4
8
12
16
20
S11
S21

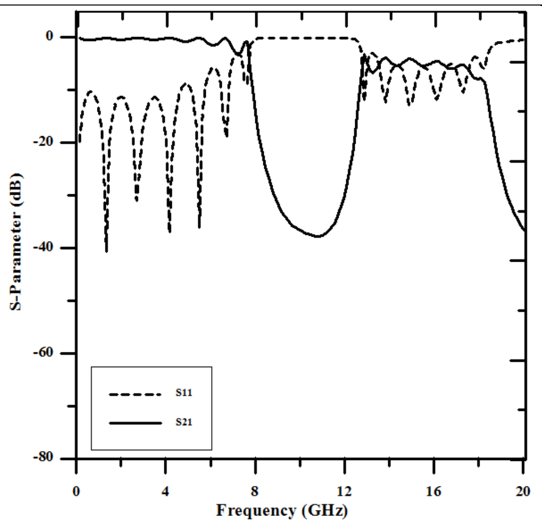
S-Parameter (dB)
Frequency (GHz)
0
-20
-40
-60
-80
0
4
8
12
16
20
S11
S21

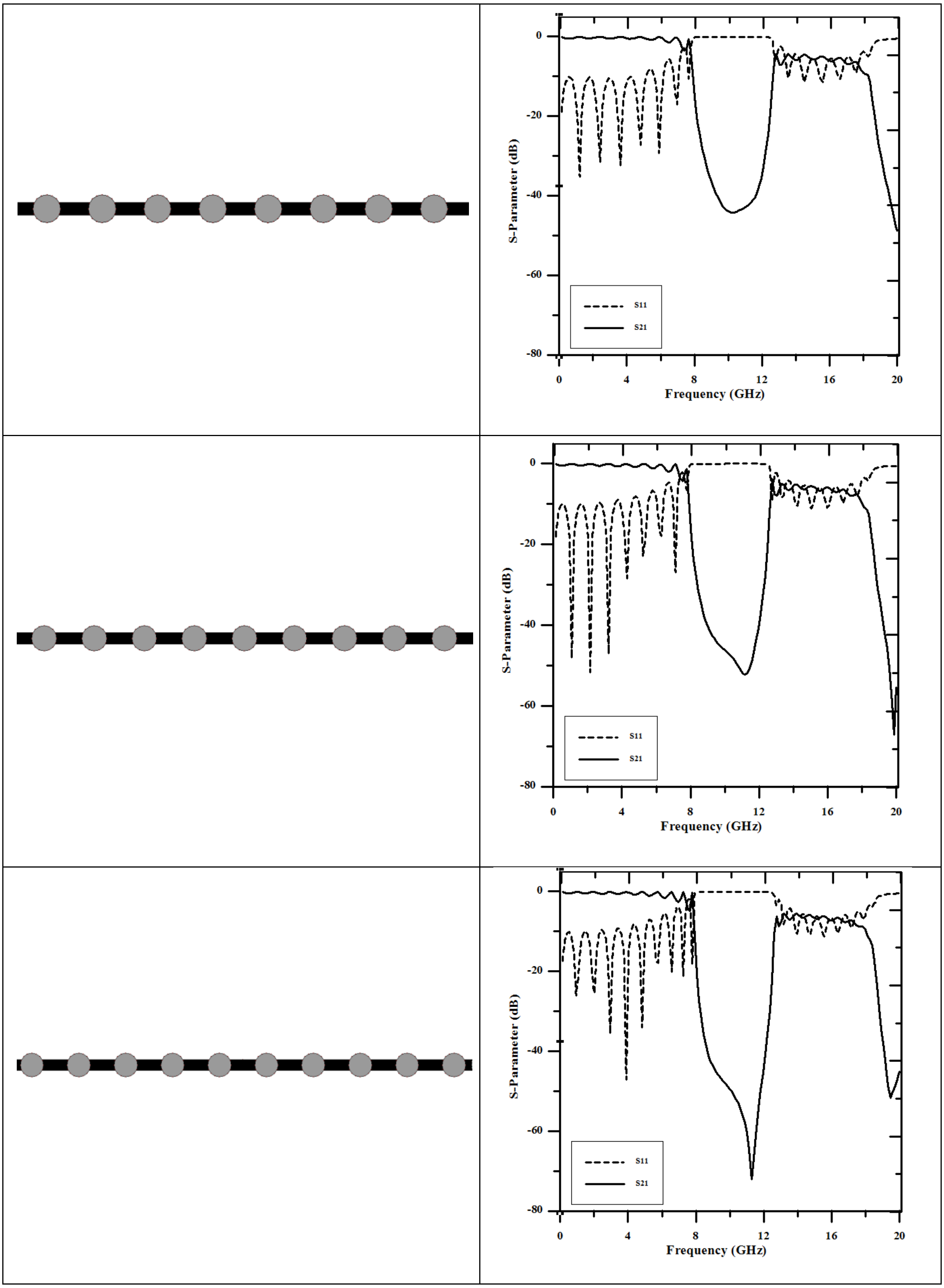

Fig 3.16. Simulated S-parameter performances of 1-D (one line) uniform circular EBGSs with 1, 2, 3, 4, 5, 6, 7, 8, 9 and 10 numbers etched over the ground plane.

So, this could be concluding that EBGSs of range 5 to 10 has given the best performance. So this range will be a follower for our further research.

3.8. Limitations of Circular or Square shaped EBGS

There are some major limitations for choosing DS-DGS instead of circular or rectangular shaped EBGS. Those are listed in the points below:

1. If the number of EBG elements increase, the passband ripple increases.
2. The passband bandwidth could not easily increase.
3. Center frequency and the cutoff frequency are higher.
4. In lower cutoff frequency range, the conventional EBGS could not perform as like DS- DGS.
5. DS- DGSs give more compact design than the conventional EBGS.

3.9. Designs of Uniform DS-DGS

Uniform DS-DGSs will also be designed. Here one row DS- DGSs will be designed. On the basis of the availability of the materials for the fabrications Taconic substrate with ε_r = 2.45 and height (h) = 31 mils is used in the simulation. The bigger slot dimension is 5.22 × 5.22 mm and narrow slot dimension is 0.72 × 1.8 mm. The geometry of 1-D (one line) DS-DGSs is shown in Figure. Here only 8 DGS elements are etched in the ground plane.

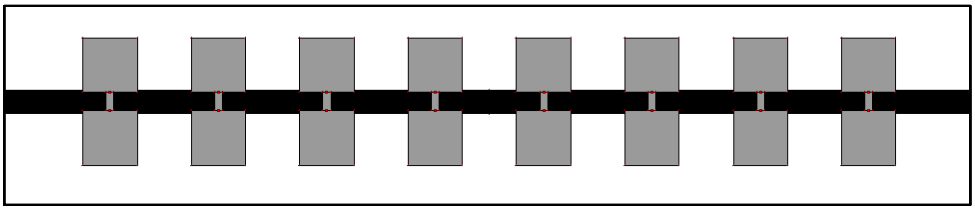

Fig 3.17. 1-D DS-DGSs patterned periodic structures under the standard 50-ohm transmission line. The substrate is Taconic having the dielectric constant of 2.45 and height of 0.787 mm. The inter-element spacing, a= 10.43 mm, element width and length, b = 5.22 mm.

- **Simulation Result of the Transmission Line with 1-D Uniform DS- DGSs**

It is mentioned that 0.5 is the optimum FF of the larger slot of DGS for Taconic with the dielectric constant of 2.45 and height of 0.787 mm. Based on this value a microstrip transmission line with 1-D uniform DS-DGSs has been investigated. The simulation result is shown in Figure.

It can be seen from the figure that this design provides wider passband and deeper stopband. The 20 dB rejection bandwidth is 2.73 GHz. The ripple height along the passband is not negligible in this time. The maximum value of isolation is found to be 59.4 dB. It looks like a low pass filter but observable harmonics is shown before 10 GHz frequency.

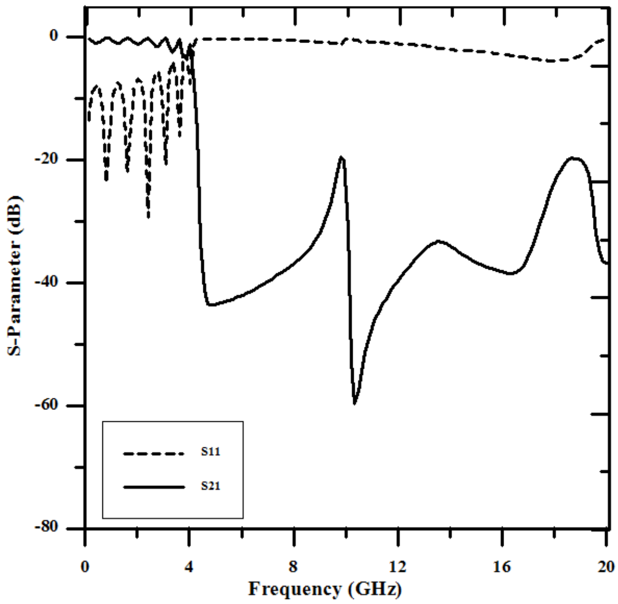

Fig 3.18. S-parameters performances of three lines uniform DS-DGS structures. The substrate is Taconic having the dielectric constant of 2.45 and height of 0.787 mm. The inter-element spacing is 10.43 mm and FF with respect to the larger element is 0.5.

3.10. Compactness

Defective Ground Structures plays a vital role to make the compact size structures. For example, the conventional circular patterned DGS structure under the transmission line makes the center frequency near about 10GHz and cutoff frequency near about 7GHz. For the lower the cutoff frequency a change is required for the design. According to the theory, it is necessary to change the filling factor (FF) either by reducing EBG areas or by increasing the interval between two EBG structures. The change is that the filling factors i.e., the interval between two EBG structures are increased.

The graphical representation of the insertion loss performances of a standard 50 ohm transmission line perturbed by 1-D (one line) uniform rectangular EBGSs vs. DS-DGS is shown below,

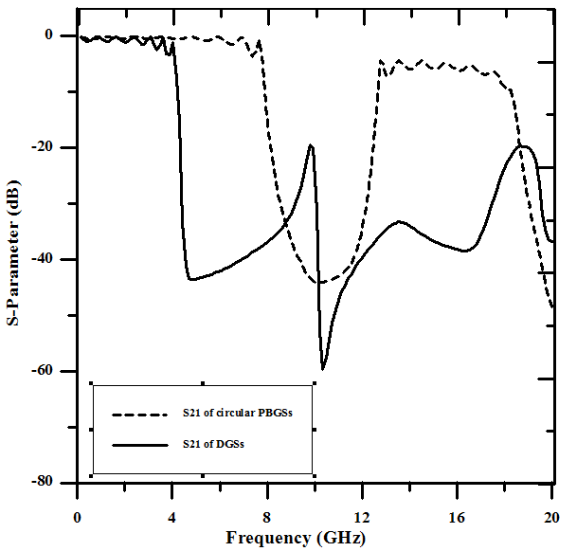

Fig 3.19. Simulated insertion loss performances of a standard 50 ohm transmission line perturbed by 1-D (one line) uniform circular EBGSs vs. DS-DGS in the ground plane of same element spacing.

The main drawbacks of that EBGS structure are:

1. The total size of the structure size is 200% increase from the conventional structure (figure 3.19)
2. The stopband is not too wide.

From the result of uniform DGSs, it can be seen that the DGSs make the same result with a cutoff frequency near about 4 GHz by the compact way and also gives wider stopband than that EBGS structure. Analyzing figure, a thing is clear that DGSs are miniaturized the total designs. And these DGSs give the significant performance.

3.11. Conclusion

Firstly, the transmission line model has been presented. To understand the properties of EBGSs the theory of EBG structures and DS-DGS structures has been presented in short extent. Since they are also periodic in nature all theories of periodic structures hold true for EBGSs. Uniform circular, square-shaped EBGSs, and DS-DGSs have been analyzed. All designs have been investigated with FF of 0.25 for circular EBGSs and 0.5 for both rectangular EBGSs are considered to be the optimum value of FF. Three rows and one row uniform EBGSs are studied to replace 2-D EBG elements by 1-D EBG elements for both the shapes. Both the designs provide very similar performances. Then similar area with different shapes, different filling factor and after that different numbers of EBG elements under the 50 ohm transmission line are simulated. Finally, we could conclude that it is preferred to use 1-D EBGSs rather than 2-D EBGSs with 5 to 10 elements and for better results and compactness using DS-structures should be recommended.

Chapter 4

Investigation into Narrower Slot of DS-DGS

4.1. Introduction

In the previous chapter, uniform circular and rectangular patterned EBGSs with optimum FFs and DS-DGSs and the optimal numbers of EBG structured elements have been addressed. High passband ripples and poor passband matching are the two serious problems of conventional uniform EBGSs. In this chapter, DS-DGSs with varying gaps are investigated. Proposed DS-DGSs improve these two problems and simplifies the filter synthesis are demonstrated. In this chapter, modified DGS structures in the form of variable structures of different patterns are proposed to investigate the improvement in S-parameters performance and it will be seen if they can be used as an ideal LPF. While the uniform distribution of the circular patterned EBG is hindered with high passband ripples near the cut-off frequency, the modified structures performed superior performances by suppressing passband ripples and producing distinct wide stopbands. The modified of the proposition is that gaps of DGSs are exploited to control the LPF response and selectivity. Hence the filter synthesis is substantially relaxed in the present approach. Since the passband ripple height increases with the FF, the uniform circular patterned EBG limits the wideband applications. Using the non-uniform distribution of EBG patterns, both passband ripple and stopband width problems are alleviated and the selectivity of the stopband of planar EBGSs increases.

4.2. Parametric Studies of DS-DGS

The influences of different dimensions of DS-DGS unit cell are presented here. The investigation of some parametric studies over different dimensions of DS-DGS is described in the literature [62]. According to the literature here is investigated the parametric studies with some other different values.

- **Influence of Dimension of Larger Slot:**

The dimensions of the larger hand of larger slot had been varied by making b = 180, 200, 220 and 240 mils. The gap and width were maintained constant for all designs having g = 30 mils and w=200 mils. The insertion loss performances of these four designs are shown in Figure. For the darker one b=180 mils, for the lighter one b=240 mils.

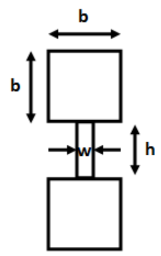

Fig 4.1. A DS-EBG structure whose length and height is b and gap width is w and gap height is h.

The cut-off frequencies are different for different dimensions. When the dimension is larger, the series inductance increases and the cut-off frequency decreases. The gap capacitance remains constant for the fixed dimension of the narrow slot. It is seen that the attenuation pole locations are also changed. This arises from the fact that the parallel combination of variable series inductance and constant shunt capacitance are always different due to changes in dimension of the larger slot. The location of the attenuation pole is the resonant frequency of an LC circuit.

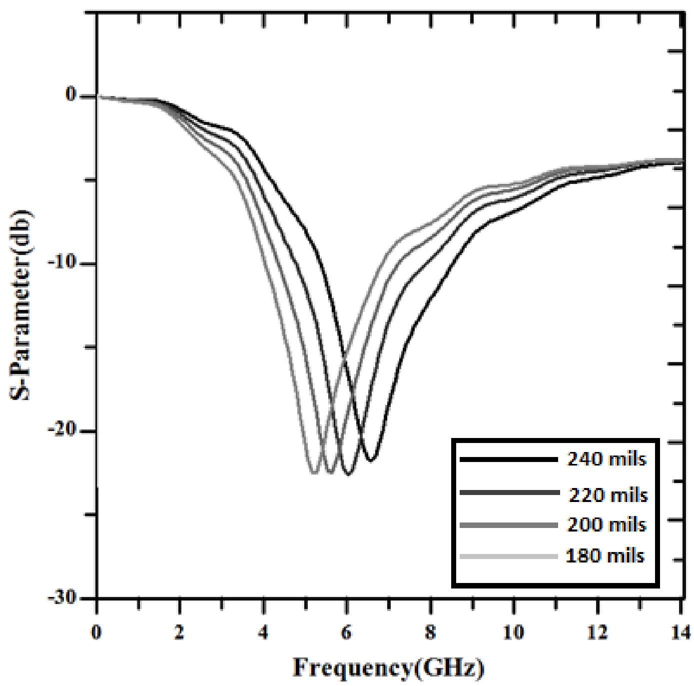

Fig 4.2. Insertion loss performance of a unit cell of DS-DGS with variable larger slots of 240, 220, 200 and 180 mils respectively.

- **Influence of the Gap-width of Narrow Slot:**

Widths were varied by making w = 20, 30, 40 and 50 mils. The dimension of the larger hand of the rectangular slot, b = 104 mils and the width of the narrow slot, h = 50 in all four designs. The Insertion loss performances are shown in figure. For the darker one, w = 20 mils, for the lighter one, w = 50 mils.

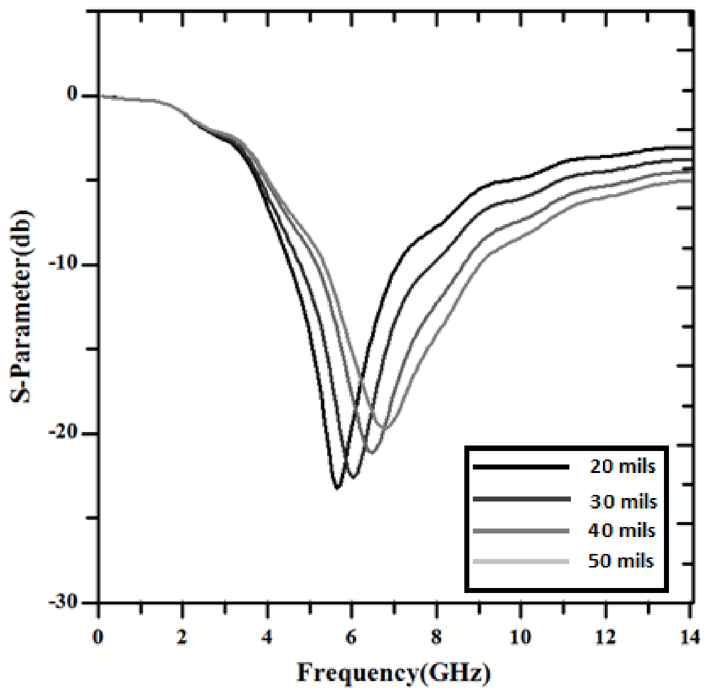

Fig 4.3. Insertion loss performance of a unit cell of DS-DGS with variable widths of 20, 30, 40 and 50 mils respectively.

It can be seen that the cut-off frequencies are approximately the same. That means the gap distance has no significant influence on the series inductance. Rather, it controls the pole location. As the gap distances are increased the gap capacitance decreases and hence the pole location moves up to a higher frequency.

- **Influence of Gap-height:**

The height of the narrow slot was varied. The effect of increasing the height is supposed to provide more capacitance as the increase in the dimension of the slot is perpendicular to the microstrip line. On the other hand, the inductive effect will also be significant. It is seen that both the pole location and the cut-off frequencies are influenced by the height of the narrow slot as expected. Increasing height enhances the inductive and capacitive effect. The insertion loss performances with different heights of a unit DGS cell are shown in figure.

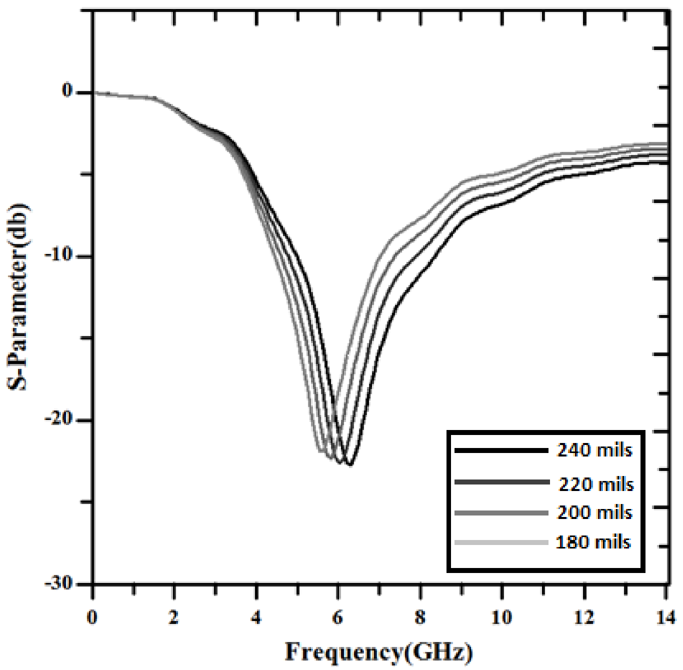

Fig 4.4. Insertion loss performance of a unit cell of DS-DGS with a variable height of narrow slots of 240, 220, 200 and 180 mils respectively.

For the darker one b=180 mils, for the lighter one b=240 mils. Based on these parametric studies the next investigation will be preceded. The objective is to describe some modified DS-DGSs and hybrid DGSs with the help of the above studies.

4.3. Proposed DS-DGSs

It is started from a conventional 1-D square patterned periodic DS-DGS structure based on Bragg's condition [60]. The original design is modified to achieve the performance of a LPF. Zealand IE3D EM software is used for simulating all the designs. The performances of different designs in terms of -20 dB cut off frequency and depth and width of stopband are investigated. The following designs are investigated are described below.

- **Design 1**

In this design, Taconic substrate having dielectric constant 2.45 and height of 0.787 mm have used. The uniform DS-DGS elements have the period of 10.43 mm. DS-EBGS is formed by etching ground plane. Two bigger slot of each cell is square shaped having the dimension of 5.22 mm. Narrower slot length is 0.75 mm and width 1.78 mm. Four dumbbell cells have formed the EBG structure in the ground plane shown in the figure below.

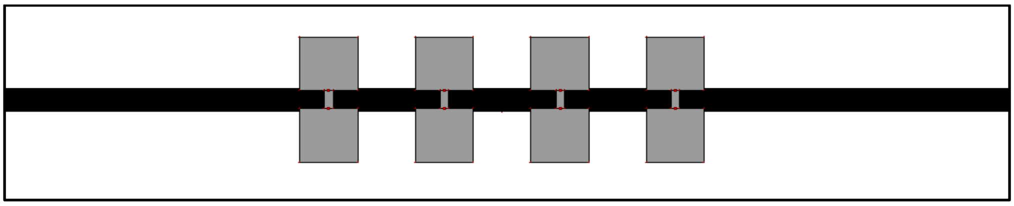

Fig 4.5. Geometry of a DS-EBGS on the ground plane of T line. The periodicity of EBGS= 10.43 mm. Taconic substrate has dielectric constant= 2.45 and height= 0.787 mm. Narrower slot length 0.75 mm and width 1.78 mm.

Insertion loss parameter S21 and return loss parameter S11 of this design are shown in the figure. The -20 dB cut off frequency of design 1 is 5 GHz. After 4 GHz the slope of insertion loss curve goes down sharply. -20 dB insertion loss bandwidth is 13 GHz. The depth of stopband is -42 dB.

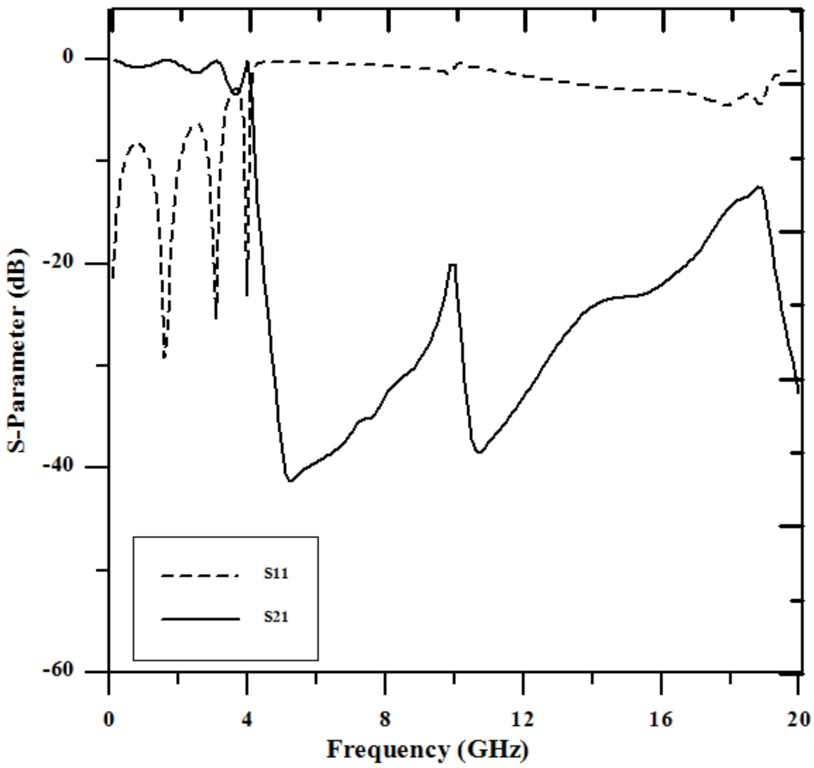

Fig 4.6. S parameter performance of DS-EBGS on the ground plane of T line according to design.

- **Design 2**

In this design dumbbell shape, EBGS is formed by etching ground plane. Two bigger slot of each cell is square shaped having the dimension of 5.22 mm. Narrower slot length is 0.75 mm and width 1 mm. Four dumbbell cells have formed the EBG structure in the ground plane shown in the figure below.

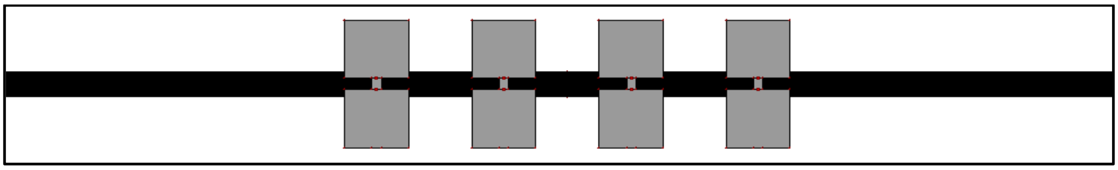

Fig 4.7. Geometry of a DS-EBGS on the ground plane of T line. The periodicity of EBGS= 10.43 mm. Taconic substrate has dielectric constant= 2.45 and height= 0.787 mm. Narrower slot length 0.75 mm and width 1 mm.

Insertion loss parameter S21 and return loss parameter S11 of Design 2 are shown in the figure. The -20 dB cut off frequency of design 2 is 5GHz. After 4 GHz the slope of insertion loss curve goes down sharply. -20 dB insertion loss bandwidth is 13.2 GHz. The depth of stopband is-51dB.

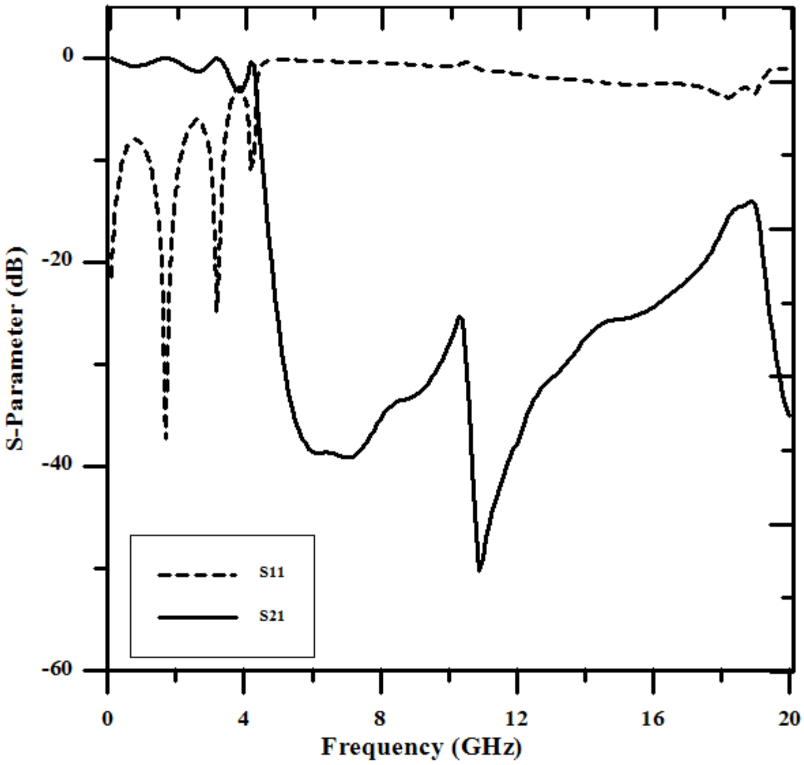

Fig 4.8. S Parameter performance of DS-EBGS on the ground plane of T-line according to design.

- **Design 3**

In this design dumbbell shape, EBGS is formed by etching ground plane. Two bigger slot of each cell is square shaped having the dimension of 5.22 mm. narrower slot length is 0.75 mm and width 0.78 mm. Four dumbbell cells have formed the EBG structure in the ground plane shown in the figure below.

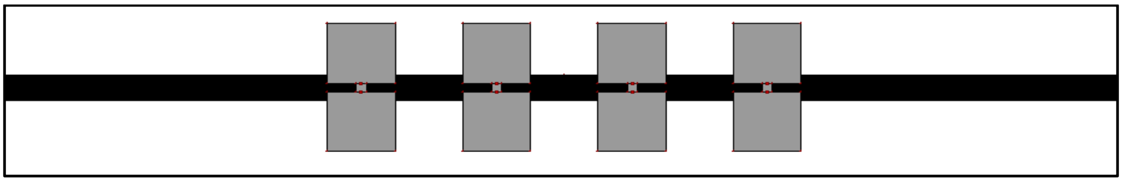

Fig 4.9. Geometry of a square shape EBGS on the ground plane of T line. The periodicity of EBGS= 10.43 mm. Taconic substrate has dielectric constant= 2.45 and height= 0.787 mm. Narrower slot length 0.75 mm and width 0.78 mm.

Insertion loss parameter S21 and return loss parameter S11 of Design 3 are shown in the figure. The -20 dB cut off frequency of design 3 is 5GHz. After 4 GHz the slope of insertion loss curve goes down sharply. -20 dB insertion loss bandwidth is 13.8 GHz. The depth of stopband is-52 dB.

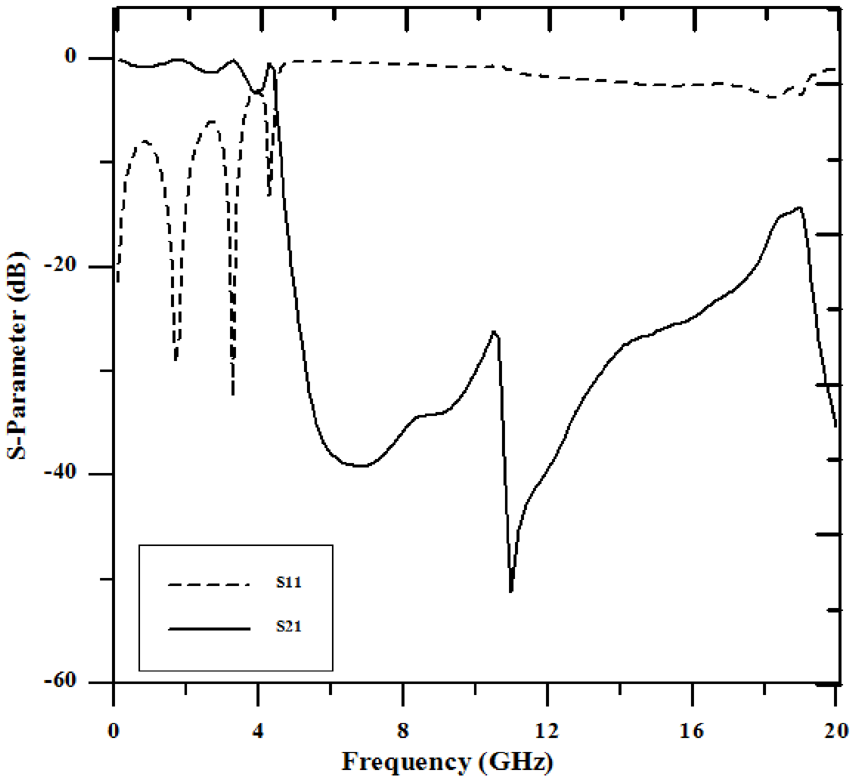

Fig 4.10. S parameter performance of DS-EBGS on the ground plane of T line according to design.

- **Design 4**

In this design dumbbell shape, EBGS is formed by etching ground plane. Two bigger slot of each cell is square shaped having the dimension of 5.22 mm. Two narrower slot lengths are 0.75 mm and width 0.78 mm. Four dumbbell cells have formed the EBG structure in the ground plane shown in the figure below.

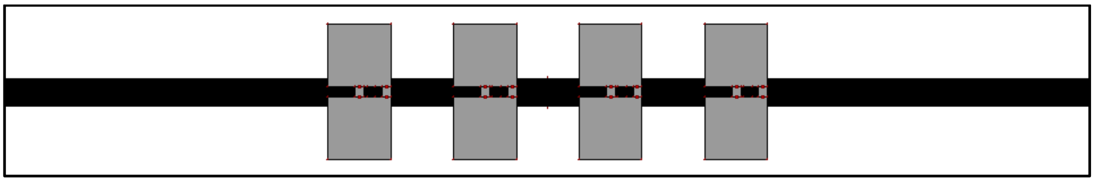

Fig 4.11. Geometry of a square shape EBGS on the ground plane of T line. The periodicity of EBGS= 10.43 mm. Taconic substrate has dielectric constant= 2.45 and height= 0.787 mm. Narrower slots length 0.75 mm and width 0.78 mm.

Insertion loss parameter S21 and return loss parameter S11 of Design 4 are shown in the figure. The -20 dB cut off frequency of design 4 is 5GHz. After 4 GHz the slope of insertion loss curve goes down sharply. The depth of stopband is -45 dB.

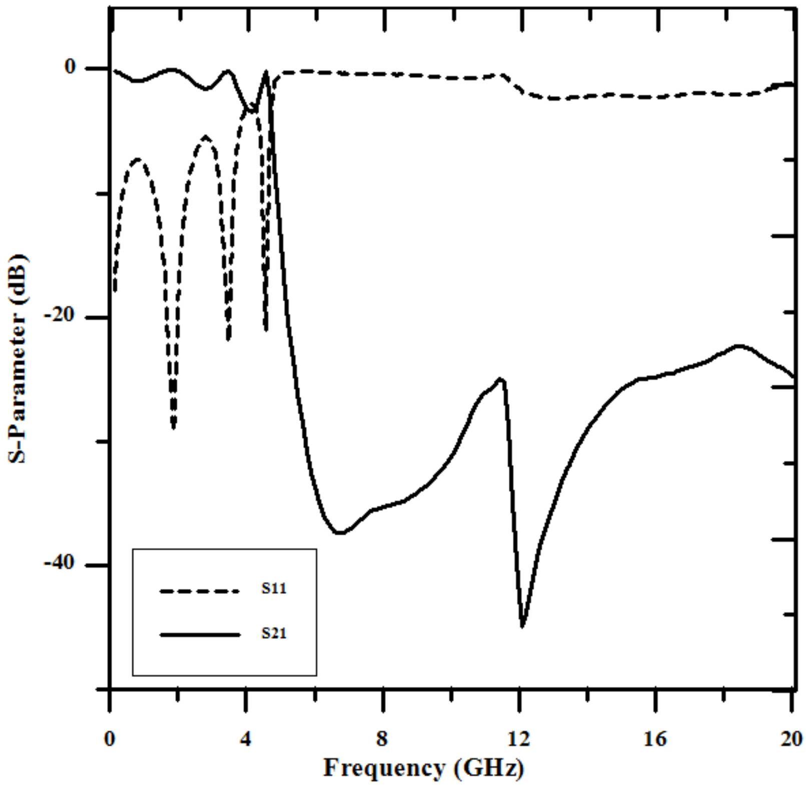

Fig 4.12. S parameter performance of DS-EBGS on the ground plane of T line according to design.

- **Design 5**

In this design dumbbell shape, EBGS is formed by etching ground plane. Two bigger slot of each cell is square shaped having the dimension of 5.22 mm. Two narrower slot lengths are 0.75 mm and width 0.78 mm. Four dumbbell cells have formed the EBG structure in the ground plane shown in the figure below.

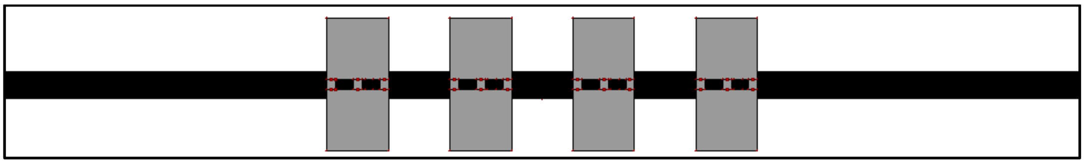

Fig 4.13. Geometry of a square shape EBGS on the ground plane of T line. The periodicity of EBGS= 10.43 mm. Taconic substrate has dielectric constant= 2.45 and height= 0.787 mm. Narrower slots length 0.75 mm and width 0.78 mm.

Insertion loss parameter S21 and return loss parameter S11 of Design 5 are shown in the figure. The -20 dB cut off frequency of design 4 is 5GHz. After 4 GHz the slope of insertion loss curve goes down sharply. The depth of stopband is -35 dB.

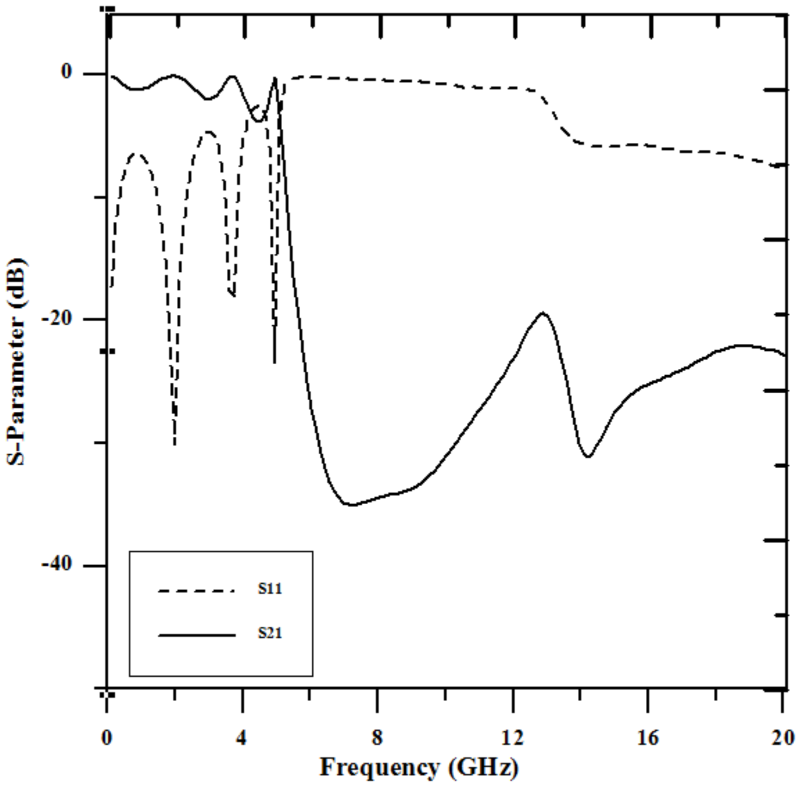

Fig 4.14. S parameter performance of DS-EBGS on the ground plane of T line according to design.

Table 4.1: Comparison of S-parameter performances of some structures.

No	Designs	S-Parameter Performance	Remarks
1.	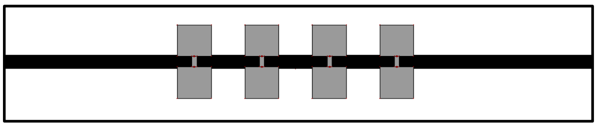	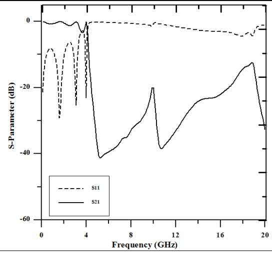	10 dB RL-BW = 4.2 GHz 20 dB IL-BW= 13 GHz Maximum ripple height= 1.5dB
2.	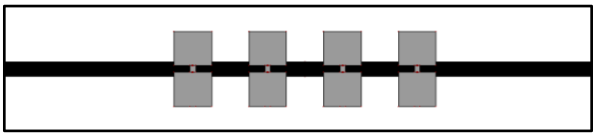	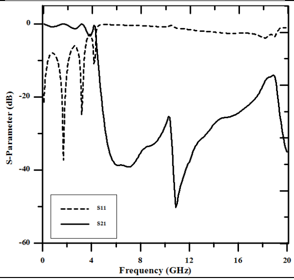	10 dB RL-BW = 4.1 GHz 20 dB IL-BW= 13.2 GHz Maximum ripple height = 1.5dB
3.	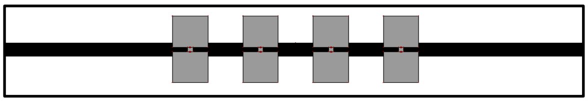	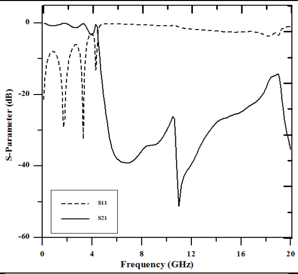	10 dB RL-BW = 4.4 GHz 20 dB IL-BW = 13.8 GHz Maximum ripple height = 1.5 dB
4.	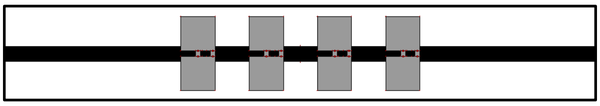	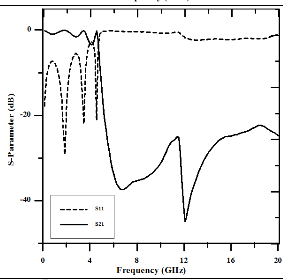	10 dB RL-BW = 4 GHz 20 dB IL-BW= 16 GHz Maximum ripple height =1.8 dB
5.	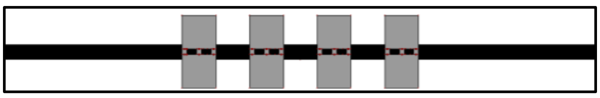	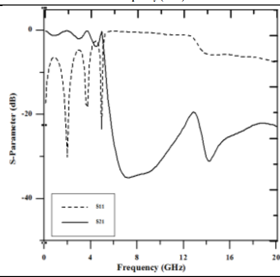	10 dB RL-BW = 4.4 GHz 20 dB IL-BW= 8 GHz Maximum ripple height = 2 dB

4.4. Fabrications

Some designs are fabricated among the designs of the thesis. Due to unavailability of VNA we could not measure the results. The fabricated designs are shown below. The design details are mentioned earlier corresponding to design numbers.

Table 4.2: Fabrication of DS-DGS assisted 50Ω transmission line

<table>
<tr><th colspan="2">Design no.</th><th>Zeland Design</th><th>Fabricated Design</th></tr>
<tr><td>1</td><td rowspan="5">Bottom View</td><td>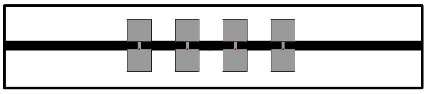</td><td>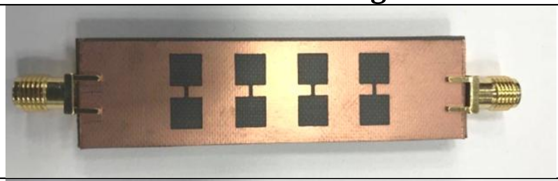</td></tr>
<tr><td>2</td><td>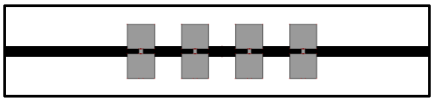</td><td>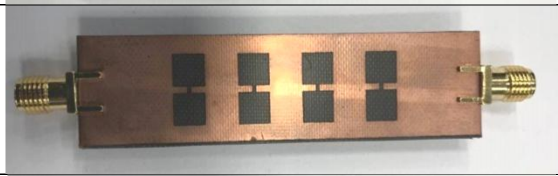</td></tr>
<tr><td>3</td><td>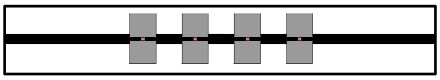</td><td>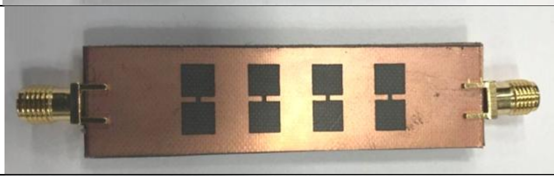</td></tr>
<tr><td>4</td><td>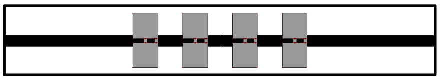</td><td>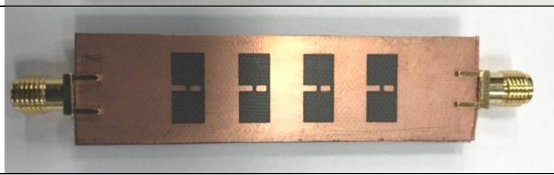</td></tr>
<tr><td>5</td><td>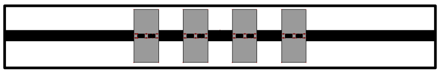</td><td>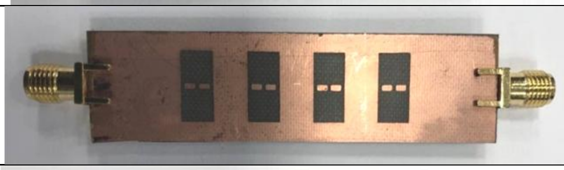</td></tr>
<tr><td colspan="2">Transmission Line
(Top View)</td><td>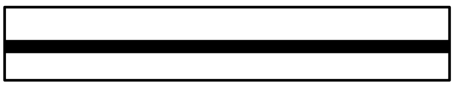</td><td></td></tr>
</table>

4.5. The validity of the simulation results

To validate the simulation results we have given description of standard EM theory from an ideal figure, logical explanations of the identical performance of the 1-D and 2-D designs and also we have compared one of our results with one published measured result. All the explanation with proper reasoning to validate our works are given below.

- **Transmission line insertion loss theory and result**

The characteristic of an ideal transmission line is that if the signal enters into the ideal transmission line, the output we get is exactly the same as the input signal. From the figure of insertion loss performance of the transmission line, it is clear that our simulation is validated.

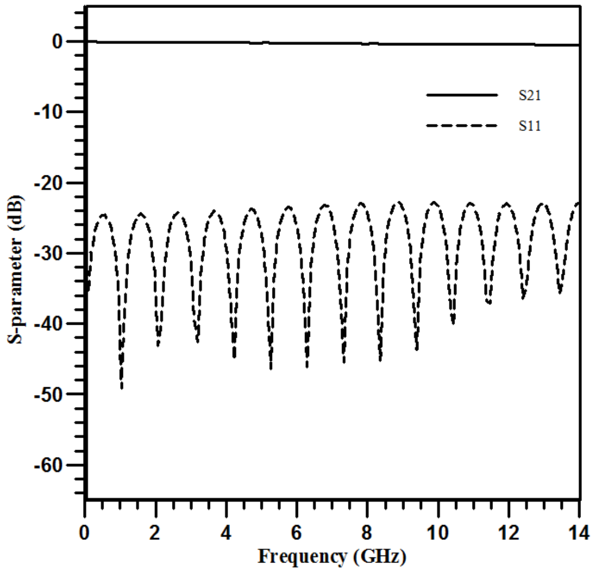

Fig 4.15. IE3D simulated S-parameter performance of an ideal 50-ohm transmission line.

- **Identical performances of 1-D and 2-D designs**

From the investigation, we have seen that 1-D and 2-D designs both give almost the similar performance. So we choose 1-D designs for the miniaturization or compactness of designs. The S-Parameter performances of 2-D and 1-D circular shaped EBGSs are given below.

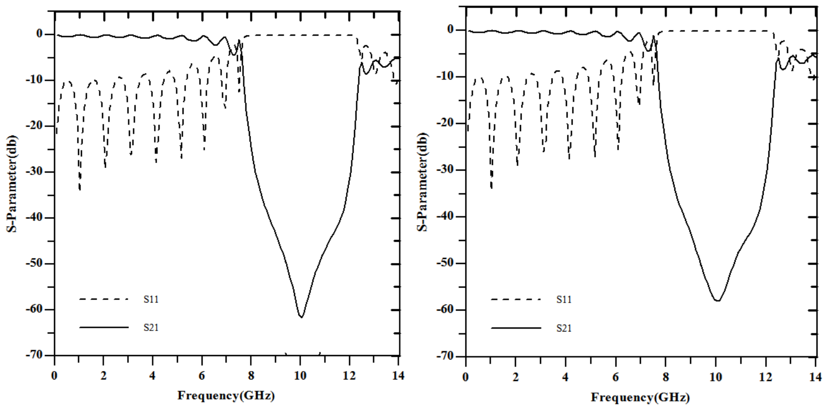

Fig 4.16. Simulated S-parameter performances of a standard 50- ohm transmission line perturbed by 2-D (three lines) (left) and 1-D (one line) (right) uniform circular EBGSs in the ground plane.

- **Validation of the measured result with software simulated result.**

For validating our software result, the one of the measured result [69] has been chosen and with the same design we have simulated our output and compare both results. One of the designs form the journal which has the measured result is redrawn by Zeland IE3D below.

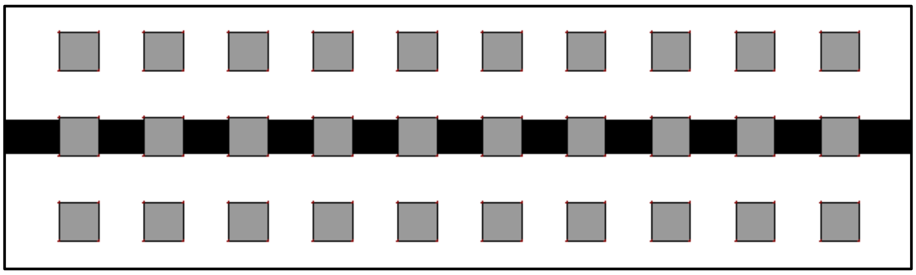

Fig 4.17. 2-D (three lines) of square patterned EBGSs under standard 50 ohm transmission line according to a published work [69].

This is the conventional 2-D square patterned EBG under 50 ohm transmission line. Inter element spacing is 226 mils. The filling factor is 0.46 and the arm length of the square EBGs are 104 mils. The geometry generated by Zeland IE3D is shown in figure.

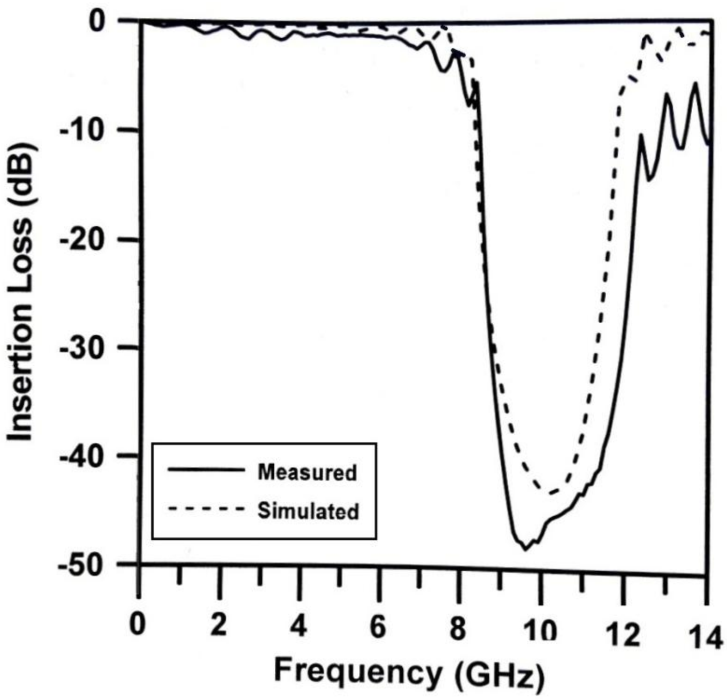

Fig 4.18. Measured and simulated result of 2-D square shaped EBG Structure for validification of result.

From the results of above figure it can clearly conclude that the measured result is identical to our software simulation result. This proves the validification of the software simulation.

4.6. Summary

In this chapter the frequency properties of the unit cell of a DS-DGS and the whole modified structures based upon the properties have been investigated. In DGS the dimension of larger square patterned slots, controls the cutoff frequencies and the gap distance controls the location of attenuation pole. Various DGS designs have been etched in the ground plane of a standard 50-ohm transmission line to develop a filter and it turns into a low pass filter (LPF). At first, few structures are investigated to yield better LPF performance in terms of passband return loss BW, less ripple transmission and wider stopband. The structures show better performance than the conventional filters designs by EBGSs. These modified designs provide the impressive LPFs. The wider stopband can be used to mitigate the surface wave problem and suppression of spurious and leakage transmission. This structure can also find potential application in RF front-ends to isolate transmitters from receiver modules.

Chapter 5

Conclusion

5.1. Introduction

The work presented in this thesis has been concerned with investigating into DS-DGS. The open literatures have been surveyed thoroughly to find their applications including their limitations. EBGSs are periodic in nature. Theories of periodic structures have been reviewed to understand the passband-stopband natures and their performances [55]. The depth and width of the stopband depend on a few factors like FFs, number of elements, periods and substrate properties. Uniform circular and square patterned EBGSs and DS- DGS have been investigated. The stopband-passband properties are reported by S-parameters performances. Different shapes of the EBG elements and structures have been shown. Three rows (2-D) of circular and rectangular uniform EBGSs under the standard 50-ohm transmission line have been simulated. Comparing with the result of one row (1-D) circular uniform circular EBGSs it is found that those three rows of uniform circular EBGSs and one row of uniform circular EBGSs yield very identical S-parameters performances. So, 1-D EBGSs have been used in whole investigation.

Next, in the chapter of conventional EBGS it is seen that if the area is same for different designs like circular or rectangular etc. the simulation result is also remains same or gives the similar performances. It is also seen that increasing the number of EBG elements enhances the stopband bandwidth. It is also investigated that the number of elements should be kept between 4 to 10. Then, the effects of FFs have been investigated. It is observed that 0.25 may be considered as the approximate value of optimized FF for circular EBGSs and 0.5 may be considered as the approximate value of optimized FF for rectangular EBGSs. There is still scope to investigate the value of optimum FF within the intermediate values ranging from 0.4 to 0.5. Finally, DS-DGS has investigated and its S-Parameter performances. And it could conclude that for achieving compactness it has no other way but choosing DS-DGS instead of conventional EBGS.

In our main proposal chapter, the parametric studies have been investigated and combined DS-DGS has been studied. Firstly, a unit cell of DS-DGS is studied. Then, the variation of larger slots of the DGS has performed and then the variations of narrower slot width and height have been performed also. From the investigation of S-parameter performances working on narrower slot have been defined. Then, from several investigations it could conclude and reported the narrower slot heights of 1.78mm, 1mm and 0.78mm. The narrower slot of 0.78mm height gives the better performance among them. Then, the investigation goes for two and three number of narrower slots between the larger slots of gap height 0.78mm. Finally, it is observed that two narrower slot designs with 0.78mm gap height gives the best performance among them.

The present research has also revealed the frequency dependence of the performance. It is important to note that frequency shifting is a common feature of EBG structures. The center frequency is controlled by the period of the EBG lattice structure that is determined from the Bragg's condition [55]. So frequency shifting can be optimized by the proper choice of period of EBGSs. Design of DS-DGSs give 4 GHz cutoff frequency where the conventional design of EBGSs gives 8 GHz cutoff frequency. So, both wider stopband and lower frequency could be obtains for using DS-DGSs.

In the simulation results, conductor loss, substrate loss and the loss due to connectors are not included. Above all, all the simulations have been done on an infinite ground plane (ignoring truncation). All the structures are fabricated using a milling machine. So there are fabrication errors. This type of error may cause variations in size and period of the lattice structures resulting in the variation in the magnitude of S-parameters and the frequency of interests. Several designs have been investigated to achieve the better performance and it has finally got the LPF performance. In terms of passband ripple height, isolation, passband return loss BW and stopband it can be concluded that these modified designs are more reliable to reach the destination.

5.2. Fulfilling the Goal of the Thesis

EBG assisted microstrip transmission line has been designed and investigated theoretically [2, 55]. The overall performance of the proposed model is always superior to conventional EBG structured transmission line. The present work has been extended further when working on narrower and larger EBG elements of DS-DGS is done on the basis of changing the gap length and width. It is pleasant to observe that simple change in the design provides enormous rejection bandwidth. In chapter 3, conventional EBGSs have been reported. Few works on DS-DGSs are found in the open literature. In chapter 4, some parametric studies of DGSs have been accomplished. Among them the effect of the width of the narrow connecting vertical slot of DS-DGS is modified investigation. And finally, proposed designs have been presented with improved performance. Thus the goal of the thesis is perfectly achieved.

5.3. Potential for Future Work

In the whole research work, attention has been paid to simulate all the structures by commercial EM software Zeland IE3D. The future work can be mentioned in the following manner. The EBGSs are actually complex geometries. For such geometries it is a difficult task to calculate the value of the propagation constant. The future task could be reducing the complexity of geometry. VNA can measure the s-parameter performances of the EBGS structures. Investigations need to be justified experimentally by VNA and compared with simulated results. Theoretical modeling is to be made for rectangular, circular EBGS and DS-DGS. Other complex designs like dual T-line designs need further research work to explain the behavior theoretically as well as multiple T-lines need to be considered.

Researching proper algorithms with mathematical modeling for designing DS-DGS is left for further work. Currently there is no such direct method of calculating correct parameters or correct size of DS-EBGS for designing a filter for a particular predefined performance i.e. for a particular type of dual band performance how a DS-DGS can be chosen. This could be a great opportunity for researchers who are interested in investigating EBG structures.

References

[1] E. Yablonovitch, “Inhibited spontaneous emission in solid-state physics and electronics,” *Phys. Rev. Lett.*, vol. 58, no. 20, pp. 2059 - 2063, May, 1987.

[2] L. H. Weng, Y. C. Guo, X. W. Shi, and X. Q. Chen, “An overview on defected ground structure,” *Prog. Electromagn. Resea. B,* vol. 7, pp.173–189, Aug., 2008

[3] D. Sievenpiper, L. Zhang, R. F. J. Broas, N. G. Alexopolous, and E. Yablonovitch, “Highimpedance electromagnetic surfaces with a forbidden frequency band,” *IEEE Trans. Microw.Theory Tech.*, vol. 47, no.11, pp. 2059-2074, Nov. 1999.

[4] K-C. CHEN, C-K. C. TZUANG, Y. Qian and T. Itoh “Leaky properties of microstrip above a perforated ground plane,” in *IEEE MTT-S International Microwave Symposium Digest*, Anaheim, CA, 1999, pp. 69-72.

[5] [Y. Qian, R. Coccioli, D. Sievenpiper, V. Radisic, E. Yablnovitch and T. Itoh, “Microstrip patch antenna using novel photonic band-gap structures,” *Microw. J.*, vol. 42, no. 1, pp. 66-76, Jan. 1999.

[6] R. Coccioli, F-R. Yang, K-P Ma, and T. Itoh, “Aperture-coupled patch antenna on UCPBG substrate,” *IEEE Trans. Microwave Theory Tech.*, vol. 47, no. 11, pp. 2123-2130, Nov.1999.

[7] R. Gonzalo, P. D. Maagt, and M. Sorolla, “Enhanced patch antenna performance by suppressing surface waves using photonic-bandgap substrates,” *IEEE Trans. Microwave Theory and Tech.*, vol. 47, no. 11, pp. 2131 – 2138, Nov. 1999.

[8] K. M. Shum, Q. Xue, C. H. Chan and K. M. Luck “Investigation of microstrip reflectarry using a photonic using a photonic bandgap structure.” *Microw. Opt. Tech. Lett.*, vol. 28, no. 2, pp. 114-116, Jan., 2001.

[9] P. S. Hui and A. Alphones, “Microstrip patch antenna with annular ring PBG,” in *Asia-Pacific Microwave Conference*,” Sydney, NSW, 2000, pp. 1347 - 1351.

[10] E. R. Brown, C. D. Parker, and E. Yablonovitch, “Radiation properties of a planar antenna on a photonic-crystal substrate,” *J. Opt. Soc. Amer. B. Opt. Phys.*, vol. 10, no. 2, pp. 404-407, Feb., 1993.

[11] S. K. Sharma and L. Shafai, “Enhanced performance of an aperture-coupled rectangular microstrip antenna on a simplified unipolar compact photonic bandgap (UC-PBG) structure,” in *IEEE Antennas and Propagation Society International Symposium*, Boston, MA, 2001, pp.498-501.

[12] Byers, I. Rumsey, Z. Popovic, and M-P-May, “Surface-wave guiding using periodic structures,” in *IEEE Antennas and Propagation Society International Symposium*, Salt Lake City, UT, 2000, pp. 342 - 345.

[13] D. Sievenpiper and E. Yablonovitch, “Eliminating surface currents with metallodielectric photonic crystals,” in *IEEE MTT-S International Microwave Symposium Digest*, Baltimore, MD, 1998. pp. 663-666.

[14] R. Kim and H.Y.D. Yang., “Surface waves and leaky waves in integrated circuit structures with planar periodic dipole loading,” in *IEEE Antennas and Propagation Society International Symposium,* Salt Lake City, UT, 2000, pp. 346-349.

[15] R. Coccioli and T. Itoh “Design of photonic band-gap substrates for surface waves suppression,” in *IEEE MTT-S International Microwave symposium digest*, Baltimore, MD, 1998, pp. 1259 - 1262.

[16] K-P. Ma, J. Kim, F-R. Yang, Y. Qian and T. Itoh, "Leakage suppression in stripline circuits using a 2-D photonic bandgap lattice," in *IEEE MTT-S International Microwave symposium digest*, Anaheim, CA, pp.73-76, 1999.

[17] P. De Maagt, R. Gonzalo, J. Y. Vardaxoglou, "Review of electromagnetic bandgap technology and applications", *The Rad. Sci. Bull.*, no. 309, pp. 11- 25, Jun., 2004.

[18] Chul-Soo Kim, Jun-Seok Park, Dal Ahn, and Jae-Bong Lim, "A Novel 1-D Periodic Defected Ground Structure for Planar Circuits," *IEEE Microwave and Guided Wave Lett.*, vol. 10, no. 4, pp.131-133, Apr., 2000.

[19] G. A. Richard. (2010, January 29). *Bragg's Law and Diffraction* [Online]. Available: http://www.eserc.stonybrook.edu/ProjectJava/Bragg/

[20] S. M. S. Hassan, S. M. Anayetullah and M. N. Mollah, "Sinusoidal Appearance of Nonuniform Dumbbell Shape EBGSs in Microstrip Transmission Line," in *International Conference on Electrical Information and Communication Technology*, Khulna, 2014, pp. 1-5.

[21] S. M. S. Hassan, M. N. Mollah, M. A. Rashid, N. H. Ramly, and M. Othman, "Dumbbell shape EBGS structure - worth to EBG assisted microwave filter designing," in *IEEE Asia Pacific Conference on Applied Electromagnetics*, Melaka, 2012, pp. 1-5.

[22] M. N. Mollah and N. C. Karmakar, "Pure harmonic suppression of a bandpass filter using Binomially distributed photonic bandgap structures," *Microwave and Optical Tech. Lett.*, vol. 44, no. 2, pp. 194 - 196, Jan., 2005.

[23] V. Radisic, Y. Qian, R. Coccioli, and T. Itoh, "Novel 2-D photonic bandgap structures for microstrip lines," *IEEE Microwave and guided wave Lett.*, vol. 8 no. 2, pp. 69 - 71, Feb. 1998

[24] F-R Yang, K-P Ma, Y. Qian and T. Itoh "A uniplanar compact photonic-bandgap (UCPBG) structure and its applications for microwave circuits," *IEEE Trans. Microw. Theory Tech.*, vol. 47, no. 8, pp. 1509 - 1514, Aug. 1999.

[25] M. N. Mollah and N. C. Karmakar, "Investigations into nonuniform photonic-bandgap microstrip line filters," *IEEE Trans. Microw. Theory Tech.*, vol. 51, no. 2, pp. 564 - 572, Feb. 2003.

[26] M. N. Mollah and N. C. Karmakar, "Harmonic suppression of a bandpass filter using binomially distributed photonic bandgap structures," in *IEEE Antennas and Propagation Society International Symposium*, Columbus, Jul., 2003, pp. 883 - 886.

[27] A. Oliner, "Periodic structures and photonic band-gap terminology: historical perspectives", in *29th European Microwave Conference*, Munich, Ger., 1999, pp. 295 - 298.

[28] M. N. Mollah and N. C. Karmakar, "Optimum filling factor and performances of a transmission line at X-band perturbed by binomilly distributed photonic bandgap (PBG) Structure", in *IEEE Pacific Rim Conference on Communications, Computers and signal Processing*, Victoria, BC, 2003, pp. 66 - 69.

[29] J. Shumpert, T. Ellis, G. Rebeiz and L. Katehi, "Microwave and Millimeter- Wave Propagation in Photonic Band-Gap Structures," AP-S/URSI, p. 678, 1997.

[30] C.M. Soukoulis, "The History and Review of the Modelling and Fabrication of Photonic Crystals", Nanotechnology 13, 420-423, 2002.

[31] R.S. Kshetrimayum, L. Zhu, " EBG Design using FSS Elements in Rectangular Waveguide", *ACES Journal*, Vol. 21, NO. 2, 2006.

[32] D.W. Prather, S. Shi, A.Sharkawy, J. Murakowski, G.J. Schneider,“ Photonic Crystals: Theory, Applications, and Fabrication”, John Wiley & Sons, New Jersey, 2009.

[33] J. D. Joannopoulos, R. D. Meade and J. N. Winn, Photonic Crystals: Molding the Flow of Light, New Jersey: Princeton University Press, 1995.

[34] F. R. Yang, R. Coccioli, Y. Qian, and T. Itoh, “Planar PBG Structures: Basic Properties and Applications”, *IEICE Trans. Electron.*, vol. E83-C, no. 5, pp. 687 - 696, May, 2000.

[35] T. Euler, and J. Papapolymerou, “Silicon Micromachined EBG Resonator and Two-Pole Filter with Improved Performance Characteristics,” *IEEE Microwave and Wireless Components Lett.*, vol. 13, no. 9, pp. 373 - 375, Sept., 2003.

[36] H-ju Hsu, M.J. Hill, R.W. Ziolkowski, and J. Papapolymerou, “A Duroid-Based Planar EBG Cavity Resonator Filter with Improved Quality Factor”, *Antennas and Wireless Propagation Lett.*, vol. 1 no. 2, pp. 67 - 70, Feb., 2002.

[37] W. J. Chappell, M. P. Little, and L. P. B. Katehi, “High Isolation, Planar Filters Using EBG Substrates,” *IEEE Microwave And Wireless Components Lett.*, vol. 11, no. 6, pp. 246- 248, Aug., 2001.

[38] W. J. Chappell and X. Gong, “Wide Bandgap Composite EBG Substrates”, *IEEE Trans. Antennas Propag.*, vol. 51, no. 10, pp. 2744 - 2750, Oct., 2003.

[39] Rumsey, M. Piket-May and P. Kelly, “Photonic bandgap structures used as filters in microstrip circuits,” *IEEE Microwave Guided Wave Lett.*, vol. 8, no. 10, pp. 336 - 338, Oct. 1998.

[40] Y. Horii and M. Tsutsumi, “Harmonic control by photonic bandgap on microstrip patch antenna,” *IEEE Microwave Guided Wave Lett.*, vol. 9, no. 1, pp. 13 - 15, Jan. 1999.

[41] R. Coccioli, W.R. Deal, and T. Itoh, “Radiation characteristics of a patch antenna on a thin PBG substrate,” in *IEEE Antennas and Propagation Society International Symposium*, Atlanta, GA, 1998, pp. 656 - 659.

[42] T. Yun and K. Chang, “One-dimensional photonic bandgap resonators and varactor tuned resonators,” *in IEEE MTT-S International Microwave Symposium Digest*, Anaheim, CA, 1999, pp. 1629 -1632.

[43] J. C. Vardaxoglou, A. Chauraya, A. P. Feresidis and P. De. Maagt, “Tunable Metallodielectric Electromagnetic Band Gap Structures with Defects”", in *International Conference on Electromagnetics in Advanced Applications*, Torino, 2003, pp. 667 - 670.

[44] M. J. Hill, R. W. Ziolkowski, and J. Papapolymerou, “A High-Reconfigurable Planar EBG Cavity Resonator,” *IEEE Microwave and Wireless Components Lett.*, vol. 11, No. 6, pp. 255 - 257, Jun., 2001.

[45] V. Radisic, Y. Qian, R. Coccioli and T. Itoh, “Novel 2-D photonic bandgap structures for microstrip lines,” *IEEE Microwave and guided wave Lett.*, vol. 8 no. 2, pp. 69 - 71, Feb. 1998.

[46] T. Lopetegi, M. A. G. Laso, J. Hernandez, M. Bacaicoa, D. Benito, M. J. Garde, M. Sorolla and M. Guglielmi, “New Microstrip Wiggly - Line Filters with Spurious Passband Suppression,” *IEEE Trans. Microw. Theory Tech.*, vol. 49, no. 9, pp. 1593 - 1598, Sep., 2001.

[47] D. Nesic, “A New Type of Slow-Wave 1-D PBG Microstrip Structure without Etching in the Ground Plane for Filter and Other Applications,” *Microw. Opt. Tech. Lett.*, vol. 33, no. 6, pp. 440 - 443, Jun., 2002.

[48] D. Nesic, “A New Type of Slow-Wave 1D PBG Microstrip Band-Pass Filter,” *Microw. Opt. Tech. Lett.*, vol. 37, no. 3, pp. 201 - 203, May, 2003.

[49] F.R. Yang, Y. Qian and T. Itoh, “A novel compact microstrip bandpass filter with intrinsic spurious suppression,” in *Asia-Pacific Microwave Conference*, pp. 593 - 596, Dec. 1998.

[50] F.R. Yang, Y. Qian and T. Itoh, “A novel uniplanar compact PBG structure for filter and mixer applications,” *IEEE MTT-S International Microwave Symposium Digest*, Anaheim, CA, 1999, pp. 919 - 922.

[51] C. Hang, V. Radisic, Y. Qian, and T. Itoh, “High efficiency power amplifier with novel PBG ground plane for harmonic tuning,” *IEEE MTT-S International Microwave Symposium Digest*, Anaheim, CA, 1999, pp. 807 - 810.

[52] W. L. Stutzman and G. A. Thiele, “Electromagnetic BandGap Structures,” in *Antenna Theory and Design*, 3rd ed., John Wiley & Sons, 1998.

[53] F.R. Yang, R. Coccioli, Y. Qian and T. Itoh, “PBG assisted gain enhancement of patch antennas on high-dielectric constant substrate,” *IEEE Antennas and Propagation Society International Symposium*, Orlando, FL, 1999, pp. 1920 - 1923.

[54] R. Coccioli, F.R. Yang, K.P. Ma, and T. Itoh, “Aperture coupled patch antenna on UCPBG substrate,” *IEEE Trans. Microw. Theory Tech.*, vol. 47, no.11, pp. 2123 - 2130, Nov. 1999.

[55] D. M. Pozar, *Microwave Engineering.* Reading, MA: Addison-Wesley, 1990.

[56] V. Radisic, Y. Qian, and T. Itoh, “Novel architectures for high-efficiency amplifiers for wireless applications,” *IEEE Trans. Microw. Theory Tech*. vol.46. no. 11, pp. 1901-1909, Nov. 1998.

[57] T. Lopetegi, M. Laso, R. Gonzalo et al., “Electromagnetic crystals in microstrip technology,” *Optical and Quantum Electronics*, vol. 34, no. 1–3, pp. 279–295, 2002.

[58] T. Lopetegi, M. Laso, J. Hernandez, M. Bacaicoa, D. Benito, M. J. Garde, M. Sorolla, and M. Guglielmi, “New Microstrip Wiggly - Line Filters with Spurious Passband Suppression,” *IEEE Trans.Microw. Theory Tech.*, vol. 49, no. 9, pp. 1593-1598, 2001.

[59] D. Nesic, “A New Type of Slow-Wave 1-D PBG Microstrip Structure without Etching in the Ground Plane for Filter and Other Applications,” *Microw. Optic. Tech. Lett.*, Vol. 33, No. 6, pp. 440-443, 2002.

[60] D. Nesic, “A New Type of Slow-Wave 1D PBG Microstrip Band-Pass Filter,” *Microw. Optic. Tech. Lett.*, Vol.37, No.3, pp.201-203,2003.

[61] S. Rogers, W. McKinzie, G. Mendolia, “AMCs Comprised of Interdigital Capacitor FSS Layers Enable Lower Cost Applications,” IEEE AP-S Int. Symp., Columbus, OH, 2003.

[62] S. Tse, B. Sanz Izquierdo, J.C. Batchelor and R.J. Langley, “Reduced sized Cells for Electromagnetic Bandgap Structures,” *Elec. Let.*, Vol. 39 No. 24, 2003.

[63] A.P. Feresidis, G. Apostolopoulos, N. Serfas, and J. C. Vardaxoglou, "Closely Coupled Metallo the dielectric Electromagnetic Band Gap (CCMEBG) Structures Formed By Double Layer Dipole and Tripole Arrays", *IEEE Transactions Antennas and propagation*, 2004.

[64] P. Feresidis, G. Apostolopoulos and. J. C. Vardaxoglou, "Miniaturised Metallothe dielectric EBG structures", IEEE International Conference on Electromagnetics in Advanced Applications (ICEAA), Torino, Italy, pp. 671-674, 2003.

[65] G. Goussetis, A. P. Feresidis and J. C. Vardaxoglou, "Performance of Metallothe dielectric EBG Structures with Periodic Loaded Elements", Proc. IEE Seminar on Metamaterials, for Microwave and (Sub)Millimetre Wave Applications, London, UK, pp. 7/1-7/5, 2003.

[66] A.P. Feresidis, A. Chauraya, G. Goussetis, J. C. Vardaxoglou and P. de Maagt, "Multiband Artificial Magnetic Conductor Surfaces", Proc. IEE Seminar on Metamaterials, for Microwave and (Sub)Millimetre Wave Applications, London, UK, pp. 2/1-2/4, 2003.

[67] S. M. Shakil Hassan, Md. Nurunnabi Mollah, “Offset EBGS against tapered EBGS: Substantial reduction of microstrip stopband filter in size”, in IEEE Region 10 Conference (TENCON), Singapore, 2016.

[68] S. M. Shakil Hassan, Nurunnabi Mollah, Khandkar Raihan Hossain, “Observation of low-pass performance from novel trapezoidal slotted dumbbell shape EBGS”, 2nd International Conference on Electrical Information and Communication Technologies (EICT), Khulna, Bangladesh, 2016.

[69] Md. Nurunnabi Mollah and Nemai Chandra Karmakar, "Compact hybrid defected ground plane," *Microwave optic. Tech. lett.,* vol. 44, issue 3, pp. 266-270, Feb. 2005